



Measurement of exclusive pion pair production in proton–proton collisions at $\sqrt{s} = 7$ TeV with the ATLAS detector

ATLAS Collaboration*

CERN, 1211 Geneva 23, Switzerland

Received: 1 December 2022 / Accepted: 9 February 2023 / Published online: 17 July 2023
© CERN for the benefit of the ATLAS collaboration 2023

Abstract The exclusive production of pion pairs in the process $pp \rightarrow pp\pi^+\pi^-$ has been measured at $\sqrt{s} = 7$ TeV with the ATLAS detector at the LHC, using $80 \mu\text{b}^{-1}$ of low-luminosity data. The pion pairs were detected in the ATLAS central detector while outgoing protons were measured in the forward ATLAS ALFA detector system. This represents the first use of proton tagging to measure an exclusive hadronic final state at the LHC. A cross-section measurement is performed in two kinematic regions defined by the proton momenta, the pion rapidities and transverse momenta, and the pion–pion invariant mass. Cross-section values of 4.8 ± 1.0 (stat) $_{-0.2}^{+0.3}$ (syst) μb and 9 ± 6 (stat) $_{-2}^{+2}$ (syst) μb are obtained in the two regions; they are compared with theoretical models and provide a demonstration of the feasibility of measurements of this type.

1 Introduction

A significant fraction of LHC proton–proton (pp) collisions are either elastic ($\approx 25\%$) or diffractive ($\approx 20\%$ of the remaining inelastic collisions [1]). In many of these collisions the momentum transferred from the beam protons is too small (< 1 GeV) for perturbative quantum chromodynamics (QCD) to be applicable, and instead Regge theory [2, 3] is used. This involves the exchange of a non-perturbative Pomeron, a soft colour-singlet object originally introduced to keep the universality of the s -dependence of high energy total cross sections by Gribov [4], Chew and Frautschi [5] and later providing an explanation of the rise of hadronic collision cross-sections with increasing beam energy [6]. Since QCD is assumed to be universally valid, there should nevertheless be a ‘mapping’ between Regge theory and QCD in which the exchanged Pomeron is equivalent to the exchange of quarks and gluons, the fundamental quanta of QCD. In certain kinematic regions, the Pomeron can be treated approximately as a two-gluon colour-singlet state. Exclusive diffractive processes provide a clean environment to study the interactions of Pomerons, via the observation of final states involving only several hadrons and no beam-remnants except the outgoing protons.

This paper presents first measurements of the exclusive double-diffractive production of charged-pion pairs in the process $pp \rightarrow pp\pi^+\pi^-$, schematically shown in Fig. 1, using the ATLAS detector at the LHC.

The charged pions are measured with the ATLAS inner detector [7], while the outgoing protons are measured by the ALFA detector [8], comprising two tracking stations situated in the forward regions on either side of ATLAS at distances of approximately 240 m from the ATLAS interaction point (IP). The ALFA detector system was designed in the first place to determine the total pp cross section at LHC energies, as well as to measure the LHC luminosity via small-angle proton-scattering processes [9]. The use of the ALFA detectors is a distinctive feature of the present study, since the outgoing protons are directly measured, suppressing con-

Contents

1 Introduction	1
2 Experimental apparatus	2
3 Monte Carlo generators	3
4 Data taking	4
5 Data analysis	4
5.1 Event selection	4
5.1.1 Description of selections	5
5.1.2 Data selection statistics	7
5.2 Background estimation	7
5.3 Beam and ALFA modelling inefficiencies, correction procedure	8
5.4 Kinematic distributions	10
5.5 Systematic uncertainties	10
6 Results and discussion	12
7 Conclusion	12
References	13

* e-mail: atlas.publications@cern.ch

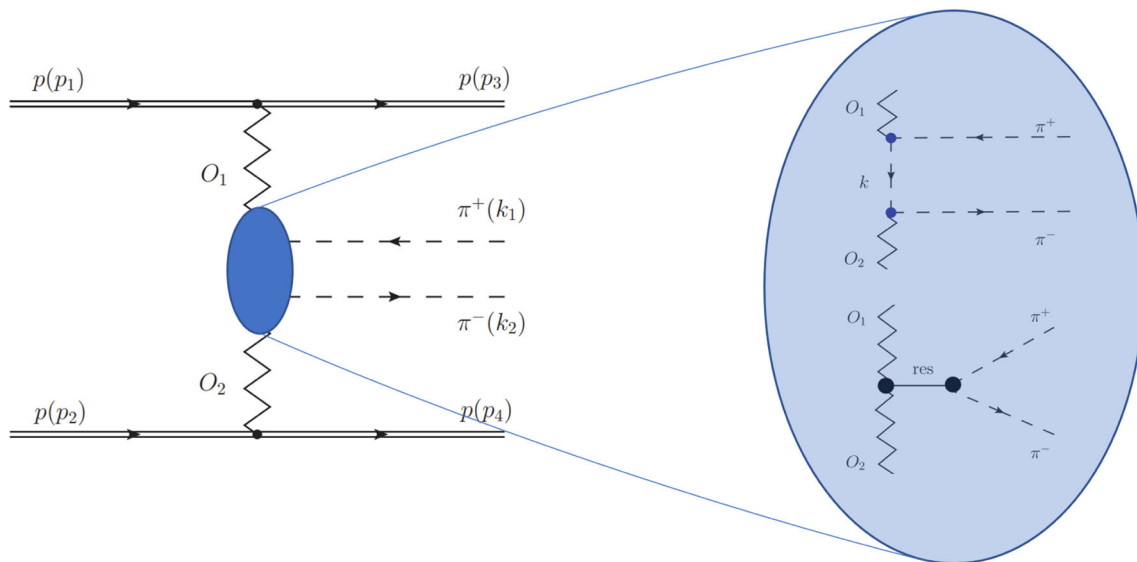


Fig. 1 A schematic Feynman diagram (left) describing the process of interest, in which two protons p with momenta p_1, p_2 interact to give a pion pair $\pi^+\pi^-$ with momenta k_1, k_2 accompanied by two outgoing protons with momenta p_3, p_4 . The exchanged virtual objects O_1 and O_2 are not necessarily of the same type, but may be typified as Reggeons

(e.g. the Pomeron) and must have all hadronic quantum numbers equal to zero. Two of the simplest examples of possible production mechanisms are shown in the bubble (right) – the upper one belonging to so-called continuum contributions and the lower one to resonance contributions

tamination from the remnants of excited scattered protons. The analysis benefits from procedures developed previously in the ALFA total cross section measurement [9].

The present results can be compared with existing measurements of the exclusive production of pion pairs using data from the ISR [10, 11], SPS [12], RHIC [13] and LHC [14, 15], where the CMS results [14, 15] are not based on purely exclusive events but on a mixture of exclusive and semi-exclusive processes. Some recent theory predictions for the process considered here may be found in Refs. [16–26]. In addition to revealing general properties of Pomerons, these channels provide a rich potential harvest for a variety of final states, including the production of resonances and the possible production of the long-sought glueball states.

2 Experimental apparatus

ATLAS is a multipurpose apparatus covering almost the entire solid angle around its LHC interaction point (IP) [7].¹ The present analysis combines information from the ATLAS

¹ ATLAS uses a right-handed coordinate system with its origin at the nominal interaction point in the centre of the detector and the z -axis along the beam-pipe. The x -axis points from the interaction point to the centre of the LHC ring, and the y -axis points upwards. Cylindrical coordinates (r, ϕ) are used in the transverse plane, ϕ being the azimuthal angle around the z -axis. The pseudorapidity is defined in terms of the polar angle θ as $\eta = -\ln \tan(\theta/2)$. Angular distance is measured in units of $\Delta R \equiv \sqrt{(\Delta\eta)^2 + (\Delta\phi)^2}$.

inner detector, the minimum-bias trigger scintillators, and the ALFA detector system.

The ATLAS inner detector (ID) [7, 27] immediately surrounds the ATLAS IP and is composed of three tracker subsystems that provide high-precision track reconstruction: a silicon pixel detector (innermost), a silicon semiconductor tracker (SCT), and a transition-radiation tracker (outermost), which also helps to discriminate electrons from hadrons. The ID covers a range of $|\eta| < 2.5$. It is surrounded by a superconducting solenoid, which produces a 2 T axial field within the ID volume.

The minimum-bias trigger scintillators (MBTS) [28] are located on either side of ATLAS between the ID and the liquid-argon calorimeter at ± 3.6 m from the IP. Each of the two MBTS detectors is oriented perpendicularly to the beam direction and consists of 16 panels assembled in two concentric rings, the outer ring covering the range $2.1 < |\eta| < 2.8$ and the inner ring covering the range $2.8 < |\eta| < 3.8$.

The ALFA detector system [8], located at $z \approx \pm 240$ m, consists of four Roman pot stations, containing vertically movable detectors that can approach the outgoing beams to within one millimetre. A schematic diagram of the detector arrangement relative to the ATLAS IP is shown in Fig. 2.

Each station is equipped with two Roman pots, each of which hosts a nearly edgeless tracking detector composed of scintillating fibres, as depicted in Fig. 3.

The ALFA detector system has a limited radiation tolerance and takes data under conditions with low numbers (μ) of

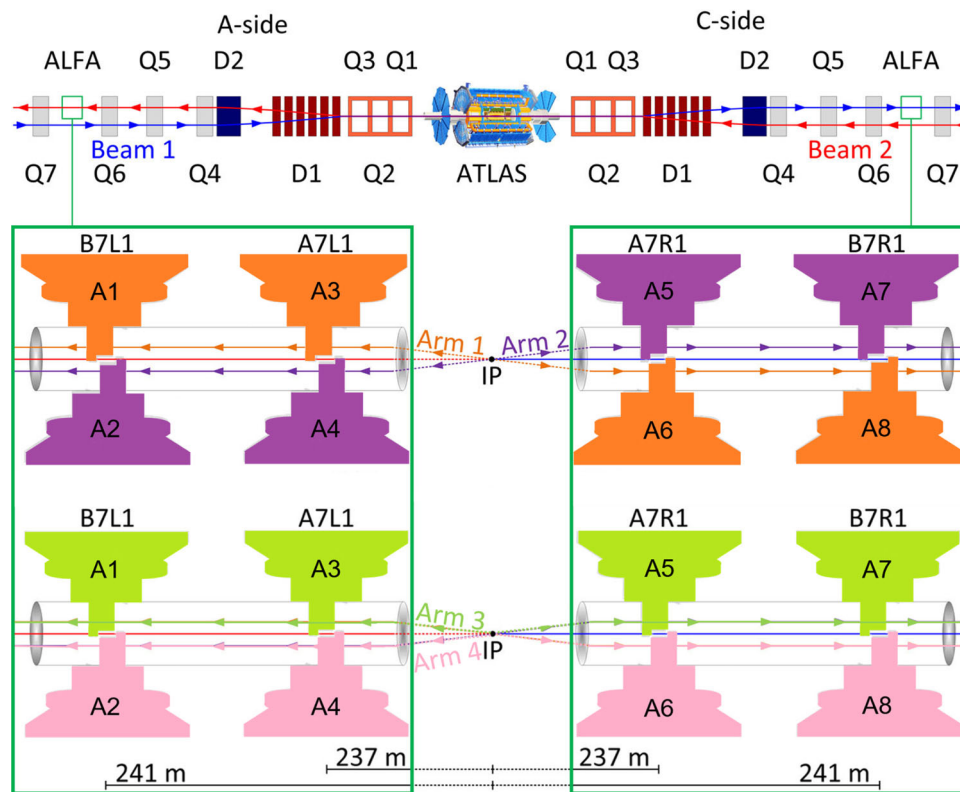


Fig. 2 A schematic depiction of the arrangement of ALFA in ATLAS, indicating the naming and numbering conventions used [8]. The upper part of the diagram gives a plan view that shows the dipole (D) and quadrupole (Q) magnets on either side of ATLAS whose settings are relevant for the beam optics. The proton beams that circulate anticlockwise and clockwise are depicted in this view, emerging into the A and C sides, respectively. The lower diagrams give side views that show the ALFA

detector combinations (arms) used for the elastic measurement (Arm 1, orange, and Arm 2, purple) and the anti-elastic measurement (Arm 3, green, and Arm 4, pink). Each arm comprises two sections (armlets), consisting of two upper or lower detectors on a single side. The ALFA stations are numbered from A1 to A8 together with a more detailed designation. In these views the vertically deflected protons entering the different arms are indicated

simultaneous proton–proton collisions interactions per beam crossing (pile-up).

An extensive software suite [29] is used in the reconstruction and analysis of real and simulated data, in detector operations, and in the trigger and data acquisition systems of the experiment.

3 Monte Carlo generators

The analysis makes use of two Monte Carlo (MC) signal generators: GENEX [30] and DIME [25].² The models are similar, but not identical, and provide different predictions. The GENEX generator is used for the baseline calculations of detection and reconstruction efficiency for the events, and for corrections to the data, while DIME is used for comparison and to estimate model uncertainties.

The generator GENEX (version May 2015) is based on a theoretical model from Lebedowicz et al. [24] and calculates the exclusive continuum production of $\pi^+\pi^-$ and K^+K^- pairs. It is based on a Regge-exchange description. The parameter determining the meson form factor (in its exponential parameterization) is the only free parameter. The implemented model describes non-resonant production without an absorption correction and does not include a rapidity gap survival factor (see e.g. Ref. [33]). In the present analysis, pions were generated within a region of pseudorapidity $|\eta| < 2.7$, and with the off-shell-pion form-factor parameter set to $\Lambda_{\text{off}} = 1 \text{ GeV}$. Otherwise, default program settings were used.

The generator DIME (version 1.06) similarly generates exclusive continuum production of $\pi^+\pi^-$ and K^+K^- pairs, although other channels are also implemented, e.g. exclusive $\rho\rho$ or $\phi\phi$ production. Unlike GENEX, DIME includes wider possibilities for modelling absorption effects: four different models (parameter *iin*, 1 – the default value used in our analysis; see Table 12 in Ref. [34]) for absorption are available

² Some other generators, also suitable for modelling the considered process, became available later, e.g. ExDiff [31] and SuperChic [32].

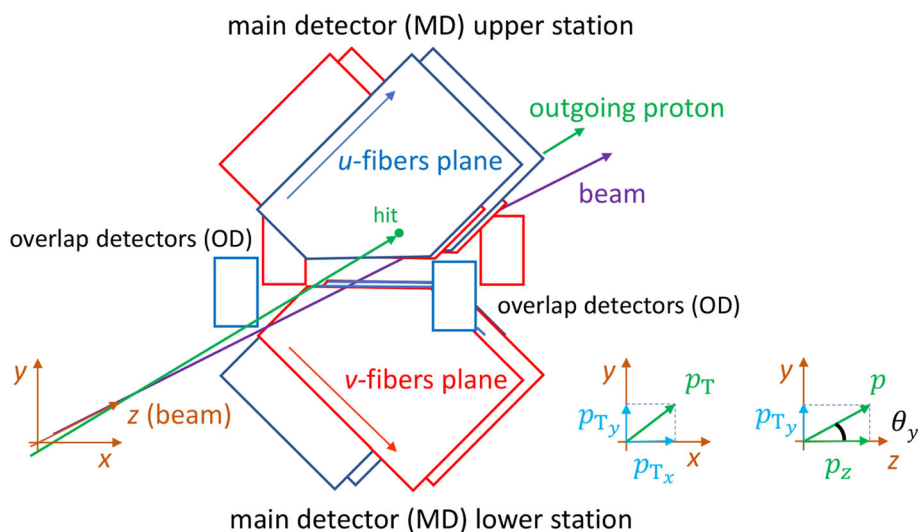


Fig. 3 A schematic drawing of the ALFA detectors in one station, here A5+A6 in Fig. 2. Each of the main detectors is made of ten u and ten v fibre layers; for more details see Ref. [8]. Only the first and last layers are drawn. For the overlap detectors, serving for the mutual positioning of the upper and lower detectors, only one of the three planes is drawn.

The trigger planes are not drawn. The local coordinate system, relative to the beamline, is indicated together with the projections of the leading outgoing proton momentum p and the angle θ_y ; the angle θ_x is defined similarly

with three different parameterizations of the meson form factor (exponential, ‘Orear-like’ – used in the present analysis, and power-like) [25].

The central diffractive background processes were generated by PYTHIA8 [35] (version 8.183), using the ATLAS A2 set of tuned parameters [36] and the MSTW2008LO PDF set [37]. PYTHIA8 employs a parton structure function approach and calculates the processes of central diffraction via double Pomeron exchange (DPE). The exclusive pion-pair process is removed from the dataset.

The GEANT4 [38] toolkit is implemented to simulate the response of the ATLAS central and forward detectors [39]. The leading outgoing protons are transported to the ALFA locations using the beam parameter values and ALFA detector positions corresponding to the data-taking period [9] in which a special high-beta* optics, referred to here as the nominal optics, was employed. The MC events were reconstructed using the same ATLAS software chain as used for the data.

4 Data taking

The data were recorded in October 2011 during a special four-hour run with high $\beta^* = 90$ m and very low pile-up given by $\mu = 0.035$. Each beam of the LHC was filled with one circulating proton bunch containing $7 \cdot 10^{10}$ protons. The integrated delivered luminosity and its uncertainty were determined to be $L_{\text{int}} = 78.7 \pm 0.1(\text{stat}) \pm 1.9(\text{syst}) \mu\text{b}^{-1}$ [9].

Two event topological configurations are used in this analysis, covering four regions of phase space. They are referred to as elastic and anti-elastic and are based on signals in different combinations of four ALFA detectors, as shown in Fig. 2. Each detector combination is designated as an arm (following the existing ALFA notation [9]), and includes detectors on side A and side C in order to measure forward protons on each side of ATLAS. The elastic configuration makes use of two arm combinations: Arm1 = arm₁₃₆₈ = A1+A3+A6+A8 (elastic arm 0) and Arm2 = arm₂₄₅₇ = A2+A4+A5+A7 (elastic arm 1), while the anti-elastic configuration uses Arm3 = arm₁₃₅₇ = A1+A3+A5+A7 (anti-elastic arm 0) and Arm4 = arm₂₄₆₈ = A2+A4+A6+A8 (anti-elastic arm 1). Each arm comprises two armlets, consisting of two ALFA stations on either the A side or C side of ATLAS. The two configurations measure different ranges of momentum transfer to the pion system and their events were recorded by different combinations of triggers during data taking. They correspond physically to different kinematic phase-space regions, and theoretical models can differ in their estimates of cross-sections.

5 Data analysis

5.1 Event selection

The event topology for exclusive pion-pair production consists of two oppositely charged pions detected by the ATLAS ID, accompanied by a leading outgoing proton entering each of the ATLAS forward regions and detected by the ALFA

Table 1 List of applied selections

Selection
Bunch selection
Lumi blocks selection
Trigger configuration
Pions:
Number of tracks
Primary vertex
ID track quality
MBTS veto
Protons:
ALFA track quality
ALFA uv -condition
ALFA clean track
ALFA geometry condition
Full system momentum balance in p_x and p_y
Fiducial region

detector system. There should be no other activity in the ATLAS ID and in the inner cells of the MBTS, and the total three-momentum of the measured protons and pions must be consistent with zero.³ The data selections are summarized in Table 1. The order in which the selections were applied to the data is given in Table 2.

5.1.1 Description of selections

The description of the conditions that are applied to select a clean sample of $pp\pi^+\pi^-$ event candidates, as summarized in Table 1, is as follows.

- Bunch system and good lumi blocks. The data come from single colliding proton bunches in the LHC. The data-recording intervals that were used ('lumi blocks') are required to be longer than 60 s in duration and the dead time must be smaller than 5%.
- Trigger. For the elastic configuration, a coincidence in the upper A-side and lower C-side detectors or the lower A-side and upper C-side detectors was required [9] (see Fig. 2). The trigger efficiency within the geometrical acceptance of the detectors is measured to be $(99.96 \pm 0.10)\%$ [9]. For the anti-elastic configuration the relevant trigger (a signal in any of the eight ALFA detectors) was prescaled by a factor of 15, which resulted in a low numbers of recorded anti-elastic events. The

³ The precise expectation value depends on the beam-crossing angle, which varied during the data taking and was at most 10μ rad in the y projection and smaller in x . The full effect is safely ignored since its impact is less than those of the ALFA detector resolution.

Table 2 Data statistics for the two configurations after the successive selection conditions. Definitions of 'arm 0' and 'arm 1' (elastic and anti-elastic) are given in Sect. 4

Selection	Configuration	
	Elastic	Anti-elastic
Recorded ATLAS events	6 620 953	
Data quality and trigger preselections	1 106 855	397 683
ID selection (pion pair)	1 520	1 115
ALFA track selection (incl. clean track and uv -condition)	486	11
MBTS veto	136	5
ALFA geometry condition	96	5
Full system momentum balance in x and y	30	3
Fiducial region	28	3
Total selected (arm 0 + arm 1)	28 (18+10)	3 (2+1)

trigger efficiency for each of the anti-elastic configurations is determined as the product of the measured single-diffractive trigger efficiencies on each side, leading to the value $(99.02 \pm 0.25)\%$ before prescaling.

- Pion system.
 - Charged tracks. Tracks in the ATLAS ID were reconstructed using a low- p_T tracking algorithm ($p_T > 100$ MeV) as in Ref. [40], where p_T denotes the transverse momentum component. Each track must pass the following quality conditions:
 - Pixel detector: at least one hit is required,
 - Semiconductor tracker: a minimum number of hits in the SCT is required, depending on the track p_T : at least two hits for $p_T > 100$ MeV, four hits for $p_T > 200$ MeV and six hits for $p_T > 300$ MeV.
- Events with at least two tracks are required. A primary vertex is required and must have exactly two accepted tracks with opposite-sign charges and small impact parameters relative to the beam axis. For the purposes of this analysis, all charged tracks are treated as pion tracks, since the numbers of electron, kaon and proton pairs are estimated to be small. The pions' transverse momenta are reconstructed [40] with an uncertainty of about 10 MeV independent of their charge.
- MBTS. To select events with no additional visible activity in the ATLAS ID, taking into consideration its limited η coverage, a MBTS veto criterion is applied: the total number of MBTS inner cells on the two ATLAS sides with a signal is required to be at most one, ignoring the outer cells. This criterion was chosen since it was robust against electronic noise in the MBTS detector.
- Proton system.

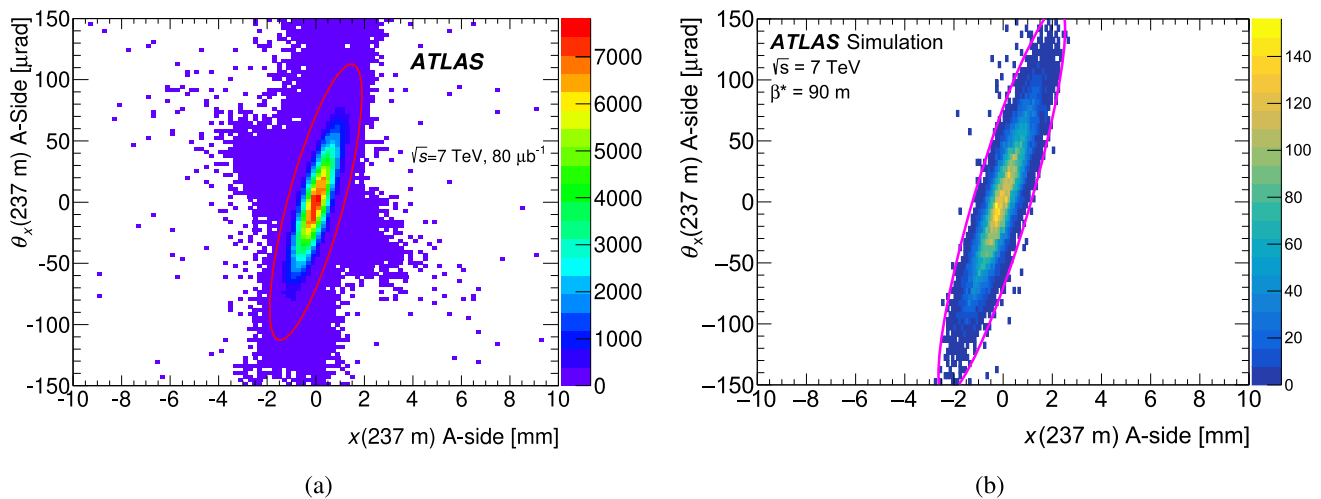


Fig. 4 The correlation between the reconstructed position of a proton at $|z| = 237$ m (A-side; a similar correlation is measured for the C-side) and its local angle projection on the horizontal direction. In **a** the proton candidates in elastic proton–proton data lie within the area of

the indicated ellipse [9]. The ellipse shown in **b** is obtained using the selection criteria applied to the sample of exclusive pion-pair production generated by GENEX

- ALFA track reconstruction. The proton reconstruction criteria used in a previous analysis [9] – bunch group, data quality, selections on the reconstructed track and geometrical deflection, beam-screen and edge conditions (see Table 2 of Ref. [9]) – together with the detector alignment, are adopted for the current study.
- ALFA uv -condition. This requirement is introduced to remove contributions from beam halo and showers (caused by interactions with material between the IP and the ALFA detectors). These contributions are absent in MC simulations. The purpose of the ALFA uv -condition is to differentiate between events with single particles and those with multi-particle showers entering the detectors, so as to filter out multi-particle signals, and in this way to allow good correspondence between MC simulations and real data samples. The uv -condition is based on the fibre multiplicities associated with a candidate proton. The first four u and first four v detector layers [8], closest to the IP, must satisfy the following:
 - at least two of these u layers, and at least two of these v layers, must have at least one hit, and
 - at most one u layer and one v layer may have more than three hits.

The first condition identifies a well-measured track and is based on the estimate of the single-fibre efficiency and a requirement on the uv -condition efficiency. The second, allowing at most two cross-talk hits surrounding that of the signal, is based on obser-

- ALFA clean track. It also rejects tracks that give rise to showers.
- ALFA clean track. Due to e.g. beam halo, pile-up or showers, more than one track may be reconstructed in a given ALFA detector [9], and it may not be possible to decide which of the tracks is the correct one. Therefore, only events with exactly one reconstructed track in each of the detectors that comprise an arm are considered in the present analysis, and a correction is evaluated for each of the configuration arms to compensate for the consequent loss of signal.
- ALFA geometric condition. In measuring leading protons, the ALFA detector system operates as a spectrometer in which a proton having a larger energy loss undergoes a larger deflection, corresponding to a larger x value of its track position measured in the horizontal direction in the coordinates of the ALFA station. In the case of exclusive pion-pair production, the energy loss of a leading proton is low and the expected distribution in the scatter plot of the reconstructed x -positions of the protons and corresponding local angles θ_x (see Fig. 3) should have a shape similar to that of elastically scattered protons. This is illustrated in Fig. 4 and allows a geometrical selection to be used to remove many protons not originating from the process of interest. Data and MC events were selected within the ellipse indicated in Fig. 4b, whose size is slightly larger than that from the elastically scattered protons shown in Fig. 4a. This covers the larger kinematic phase space occupied by the protons after losing energy to the pion system.

- Overall momentum balance. Because of the limited reconstruction of the proton kinematics, a selection criterion for overall four-momentum conservation is not possible; instead the momentum balance in the x and y projections is used.

The methods used for the reconstruction of the proton kinematics from the tracks measured by the ALFA detector are based on knowledge of the accelerator optics. As the mass of the centrally produced pion-pair system is low, the ‘lattice’ method [9], originally used for elastically scattered protons, can be applied. Proton momentum projections p_x and p_y are used in the analysis, and are reconstructed with a resolution of about 40 MeV and 1 MeV respectively.

The transverse momentum components of the full $pp\pi^+\pi^-$ system are determined with a resolution of approximately 60 MeV in p_x and 20 MeV in p_y , denoted by σ_x and σ_y respectively. The signal region is defined by $3.5\sigma_{x,y}$ intervals about zero in p_x and p_y .

- Fiducial condition. The exclusive production of pion pairs is studied within a fiducial region which is defined to be close to that which is allowed by the sub-detector acceptances. The data and Monte Carlo analyses use the same fiducial region, which is given in terms of the pseudorapidities $\eta(\pi)$ and transverse momenta $p_T(\pi)$ of the individual pions, and the mass of the central pion system $m_{\pi\pi}$:

$$|\eta(\pi)| < 2.5, \quad p_T(\pi) > 0.1 \text{ GeV},$$

$$2m_\pi < m_{\pi\pi} < 2.0 \text{ GeV}.$$

Additional conditions are applied to the y -components of the proton momenta $p_y(A)$ and $p_y(C)$, in both the elastic and anti-elastic configurations:

$$\text{armlet}_{ij}^{\text{low_cut}} < p_y(A) < \text{armlet}_{ij}^{\text{up_cut}} \quad \text{and}$$

$$\text{armlet}_{kl}^{\text{low_cut}} < p_y(C) < \text{armlet}_{kl}^{\text{up_cut}},$$

where $ijkl \in \{1368, 2457, 1357, 2468\}$ and

$$\begin{aligned} \text{armlet}_{13}^{\text{up_cut}} &= 0.267 \text{ GeV}, & \text{armlet}_{57}^{\text{up_cut}} &= 0.246 \text{ GeV}, \\ \text{armlet}_{13}^{\text{low_cut}} &= 0.080 \text{ GeV}, & \text{armlet}_{57}^{\text{low_cut}} &= 0.080 \text{ GeV}, \\ \text{armlet}_{24}^{\text{up_cut}} &= -0.079 \text{ GeV}, & \text{armlet}_{68}^{\text{up_cut}} &= -0.082 \text{ GeV}, \\ \text{armlet}_{24}^{\text{low_cut}} &= -0.250 \text{ GeV}, & \text{armlet}_{68}^{\text{low_cut}} &= -0.269 \text{ GeV}. \end{aligned}$$

These selections are evaluated in terms of the reconstructed ALFA proton kinematic parameters, calculated using the nominal beam optics and ALFA detector positions. The experimental uncertainties of these values translate into a systematic uncertainty that is common to the corrected data and the MC predictions.

5.1.2 Data selection statistics

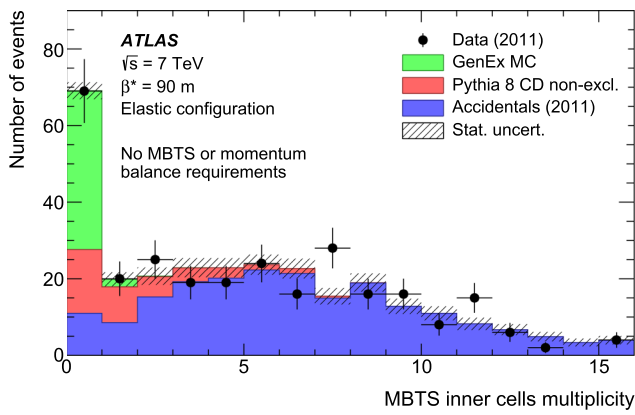
The numbers of events after the successive selection conditions are shown in Table 2.

5.2 Background estimation

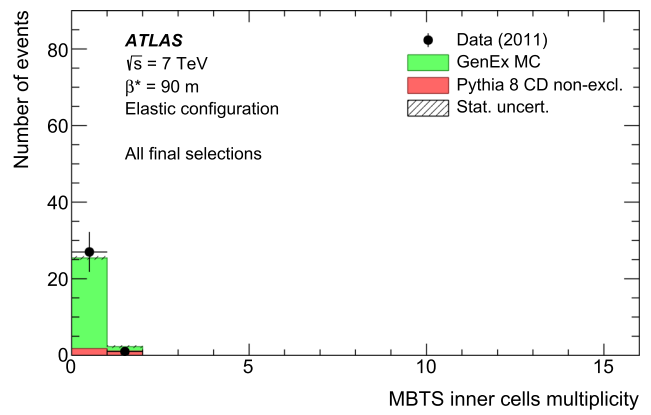
One source of background consists of centrally produced pion pairs that are accidentally accompanied by one or more beam-halo protons which are detected in ALFA. This background is suppressed by the event selections to a low level. This can be seen in Fig. 5, which shows (a) the total multiplicity distribution of the MBTS inner rings for events that satisfy the selection criteria listed in Table 1, except for those on MBTS and momentum balance, and (b) after all the selections in Table 1 are applied. A fit to the data is performed in terms of a model comprising generated signal events (GENEX) and backgrounds from (i) generated diffractive events (PYTHIA8) and (ii) an ‘accidentals’ event sample formed from data events with a pion pair that are combined with unrelated data events randomly found to have ALFA signals. For exclusive pion events, the MBTS multiplicity is at most one, while for other diffractive events it can be higher. Events with accidental coincidences can give both higher and lower MBTS multiplicities. Such events are contained in the event sample, but Fig. 5b shows that they contribute no contamination to the signal region $|p_a| < 3.5\sigma_a$, where $a = x, y$ (see Sect. 5.1.1), after all conditions listed in Table 1 are applied.

The very strong effect of the MBTS veto on background suppression is demonstrated also in Fig. 6, which shows that the summed vertical (y -axis) track momenta exhibit a clear signal peak in the total p_y of the event only after this veto is applied. Figure 6a includes events with selections up to those on the ID and ALFA tracks listed in Table 2, while Fig. 6b shows the same data and backgrounds but with the MBTS veto also applied. The background was fitted outside the signal region, which approximately covers the central three plotted intervals. The signal peak is now prominent.

Since the data were taken during the special run with very low pile-up, the remaining backgrounds, after applying the event selections of Sect. 5.1, presumably originate from other central diffraction processes. For both the elastic and anti-elastic event configurations, the backgrounds due to these diffraction processes are estimated using events satisfying the complete set of selections listed in Table 1 except for the requirement on the momentum balance in the x and y projections. They are evaluated from a fit to the p_y distribution of the data outside the signal region, using a model consisting of a background generated by PYTHIA8 and accidentals. This is shown in Fig. 7a, while Fig. 7b shows the distribution with all the selections applied.



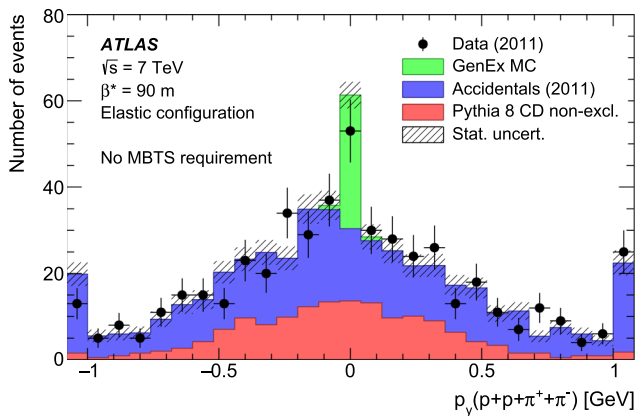
(a)



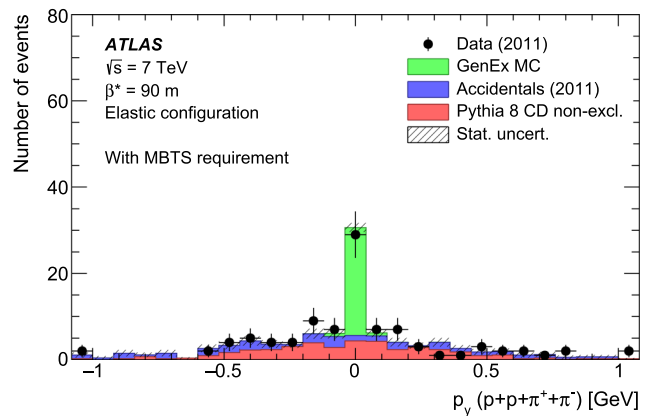
(b)

Fig. 5 Total multiplicity of the MBTS inner cells, comparing data with MC signal simulation (GENEX), MC background simulation (PYTHIA8 central diffraction (CD)), and accidental coincidences. In **a** the MBTS selection criteria and selections for momentum balance in the x and y

projections are not applied; in **b** all the selections listed in Table 1 are applied. The MC and accidental coincidences histograms are stacked. Statistical uncertainties of MC events and accidentals are combined



(a)



(b)

Fig. 6 The summed momentum values in p_y after the pion and proton system selection: **a** before and **b** after the MBTS veto is applied (see Table 2). The histograms of the MC predictions and the accidentals

are stacked. Statistical uncertainties of MC events and accidentals are combined. The underflow and overflow bins ($|p_y| > 1$ GeV) are shown

5.3 Beam and ALFA modelling inefficiencies, correction procedure

The implementation of the ALFA detector in the ATLAS simulation framework has some limitations. The response can differ from that of the real detector, mainly due to imperfect implementation of signal and noise production mechanisms and the omission of electronic cross-talk between channels.

Since the simulation does not include the production of particle showers that are due to the interaction of forward-

going particles with parts of the LHC (accelerator beam pipe, collimators, shielding of magnets, etc.), the uv -condition is introduced, effectively removing these showers from the data. This affects the signal, and the corresponding correction depends on the elastic or anti-elastic configuration ('conf') and the arm. A further correction is required for the clean track selection (Sect. 5.1).

If the MC description were perfect, the detector efficiency ϵ , for a given arm and configuration, would be written as

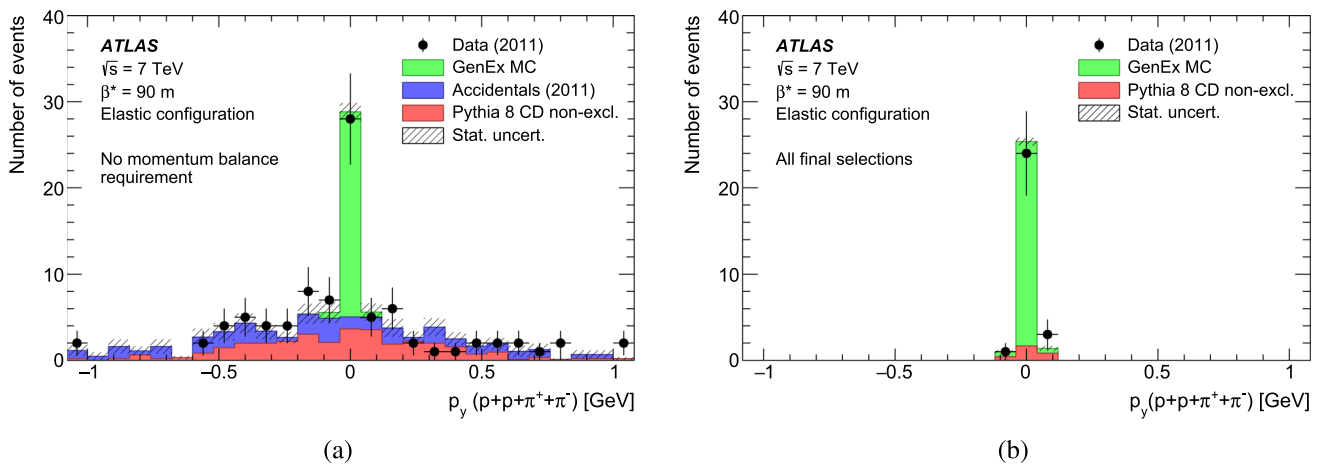


Fig. 7 Full final-state p_y momentum component of data, fitted to MC simulation and accidentals using GENEX for the signal component and a background consisting of accidentals and PYTHIA8 central diffraction (CD) without exclusive pion processes; in **a** all the final selections listed in Table 1 are applied except those on the momentum balance in the x

and y projections, while in **b** all the final selections are applied. The histograms of the MC predictions and the accidentals are stacked. Statistical uncertainties of the MC events and accidentals are combined. The underflow and overflow bins ($|p_y| > 1$ GeV) are shown

$$(\epsilon)_{\text{arm}}^{\text{conf}} = \left[\left(\frac{N_{\text{trk}}}{N_{\text{acc}}} \right)^{\text{MC}} \right]_{\text{arm}}^{\text{conf}}, \tag{1}$$

where N_{trk} is the number of generated MC signal events with at least one track reconstructed in each of the detectors in a given configuration and N_{acc} is the number of MC signal events within the acceptance of that configuration.

Since the MC simulation does not contain all relevant effects, the uv -condition and the clean track selection are introduced and Eq. (1) is now rewritten as

$$(\epsilon')_{\text{arm}}^{\text{conf}} = \left[\left(\frac{N_{\text{trk}}}{N_{\text{uv}}} \right)^{\text{data}} \times \left(\frac{N_{\text{uv}}}{N_{\text{acc}}} \right)^{\text{MC}} \right]_{\text{arm}}^{\text{conf}} \stackrel{\text{def}}{=} \left[r^{\text{data}} \times t^{\text{MC}} \right]_{\text{arm}}^{\text{conf}}, \tag{2}$$

where N_{uv} is the number of events which pass the uv -condition. The first factor in Eq. (2) is given by physics that can be mismodelled by generators, and the second factor takes account of the clean track selection.

Denoting $R_{\text{arm}}^{\text{conf}} = (o^{\text{MC}}/o^{\text{data}})_{\text{arm}}^{\text{conf}}$, where the ratio $o^X = N^X_{\text{clean}}/N^X_{\text{any}}$ gives the ratio of the number of events with clean tracks to all events in a given track sample X (MC or data), the combined correction factor $f_{\text{arm}}^{s+uv,\text{conf}}$, where $s+uv$ denotes the combination of single tracks and uv -conditions, is written as

$$f_{\text{arm}}^{s+uv,\text{conf}} = (\epsilon/\epsilon' \times R)_{\text{arm}}^{\text{conf}}$$

which, using Eq. (2), can be re-written as

$$f_{\text{arm}}^{s+uv,\text{conf}} = \left(r^{\text{MC}}/r^{\text{data}} \times o^{\text{MC}}/o^{\text{data}} \right)_{\text{arm}}^{\text{conf}}.$$

Table 3 Correction factors for the single-track selection and uv -condition, and the correction factor for MC simulation based on the GENEX generator. Statistical uncertainties are quoted

Configuration	Arm	$f_{\text{arm}}^{s+uv,\text{conf}}$	$f_{\text{arm}}^{\text{corr},\text{conf}}$
Elastic	0	1.097 ± 0.015	0.076 ± 0.001
	1	1.135 ± 0.016	0.070 ± 0.001
Anti-elastic	0	1.229 ± 0.115	0.069 ± 0.001
	1	1.126 ± 0.134	0.068 ± 0.001

Its values are given in Table 3.

The effects arising from detector efficiency and due to migrations across the fiducial phase-space boundary at particle and detector level are corrected for with a single factor for each configuration. This is adequate in view of the limited statistical precision of the data, given that the MC model describes the data well. The correction factor, $f_{\text{arm}}^{\text{corr},\text{conf}}$, is based on the GENEX MC simulation, and for a given configuration it is defined as the ratio of the number of events, $N_{\text{detector_level}}^{\text{passed}}$, that pass the event selection criteria at the detector level, to the number of events $N_{\text{particle_level}}^{\text{passed}}$ that pass the fiducial region selection at the particle level, i.e. $f_{\text{arm}}^{\text{corr},\text{conf}} = \left(N_{\text{detector_level}}^{\text{passed}}/N_{\text{particle_level}}^{\text{passed}} \right)_{\text{arm}}^{\text{conf}}$. The geometrical acceptance of each ALFA detector is ≈ 0.25 , giving rise to the calculated combined values stated in Table 3.

The visible cross-section for a given elastic or anti-elastic configuration is then determined as

$$\sigma_{\pi^+\pi^-}^{\text{vis, conf}} = \frac{1}{L} \times \left[\left(N_0^{\text{conf}} - B_0^{\text{conf}} \right) \times C_0^{\text{conf}} \right]$$

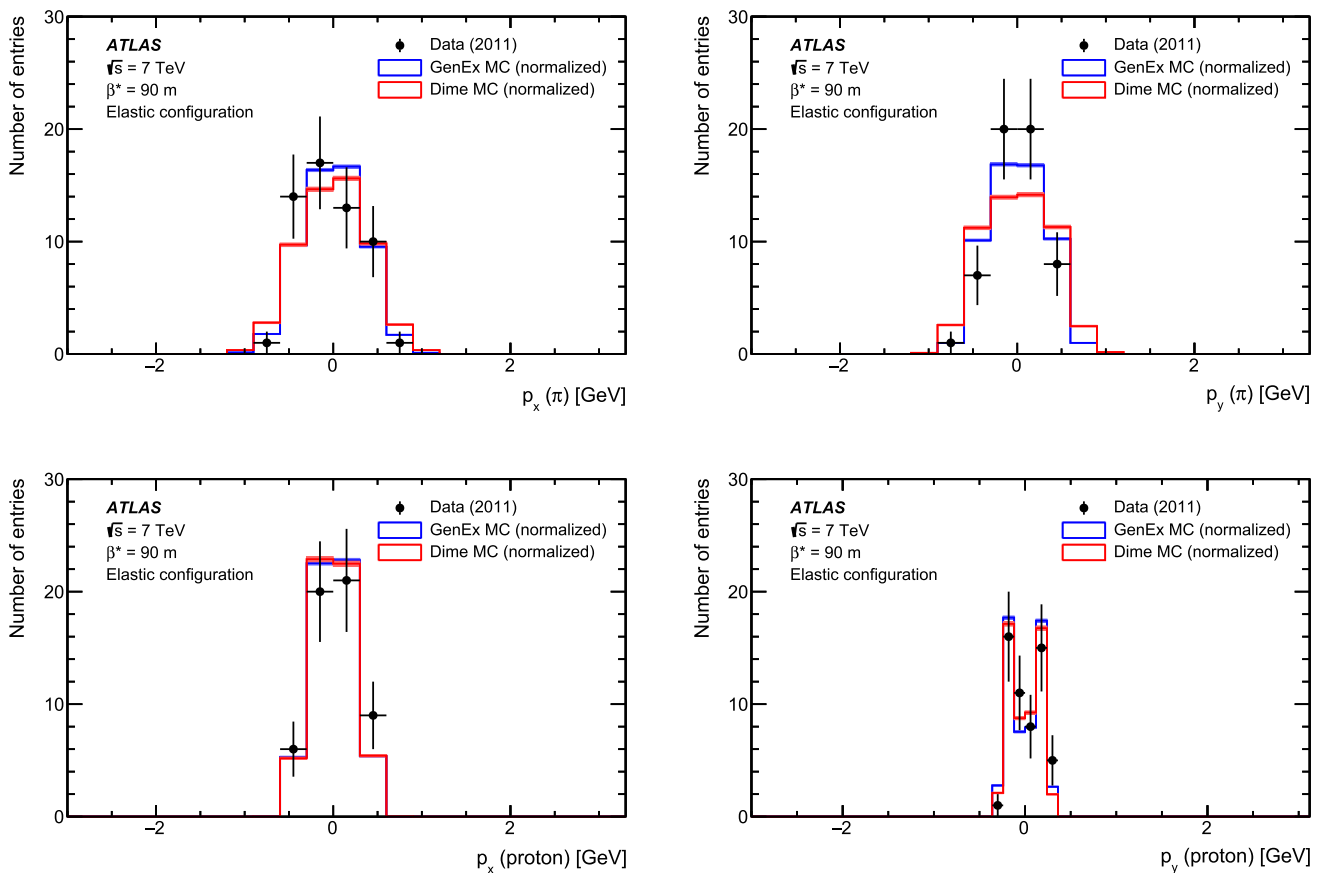


Fig. 8 Distributions, for the selected events, of p_x and p_y components of the pion tracks reconstructed in the ATLAS central detector (upper row), and p_x and p_y components of the proton tracks reconstructed in the ALFA detectors (lower row) for the data, GENEX MC and DIME

MC simulations after applying all the event selections, but without a background subtraction applied to the data ($\approx 10\%$). Each of the MC samples is scaled to the data. Statistical uncertainties are shown only for the data; they are negligible for the MC predictions

$$+ \left(N_1^{\text{conf}} - B_1^{\text{conf}} \right) \times C_1^{\text{conf}} \times \frac{1}{\epsilon_{\text{trig}}^{\text{conf}} \cdot \epsilon_{\text{DAQ}}}$$

where L represents the integrated luminosity used; $N_{\text{arm}}^{\text{conf}}$ and $B_{\text{arm}}^{\text{conf}}$ are the numbers of selected signal candidate events and calculated background events in each arm; $C_{\text{arm}}^{\text{conf}} = f_{\text{arm}}^{\text{S+uv,conf}} / f_{\text{arm}}^{\text{corr,conf}}$; $\epsilon_{\text{trig}}^{\text{conf}}$ is the trigger efficiency for the given configuration; ϵ_{DAQ} is the dead-time correction factor, as defined and determined in Ref. [9].

5.4 Kinematic distributions

Taking into account the precision of the reconstruction, the kinematic distributions of the pions and protons are well modelled by the MC simulations. Figures 8, 9 and 10 show comparisons of the distributions of the momentum components of the reconstructed pions and protons, and the pion-pair rapidity, acoplanarity, transverse momentum and invariant mass, for the data and the GENEX MC and DIME MC simulations. The distributions are presented after applying

all the event selections, but without applying a background subtraction ($\approx 10\%$) to the data. In view of the low number of events for the anti-elastic configuration, only distributions for the elastic configuration are shown.

5.5 Systematic uncertainties

The overall systematic uncertainty on the exclusive pion-pair cross-section measurement is estimated as $+6.4\%$ for the elastic configuration and -4.2% for the anti-elastic configuration. Table 4 summarizes the main sources of systematic uncertainty. The difference between the relative uncertainties of the two configurations comes mainly from data-driven systematic uncertainties. Some of the MC studies made use of slightly enlarged fiducial region criteria to estimate systematic uncertainties.

Background determination. The systematic uncertainty is determined as half of the difference between the background estimates for the standard signal region, $3.5\sigma_{x,y}$ around zero

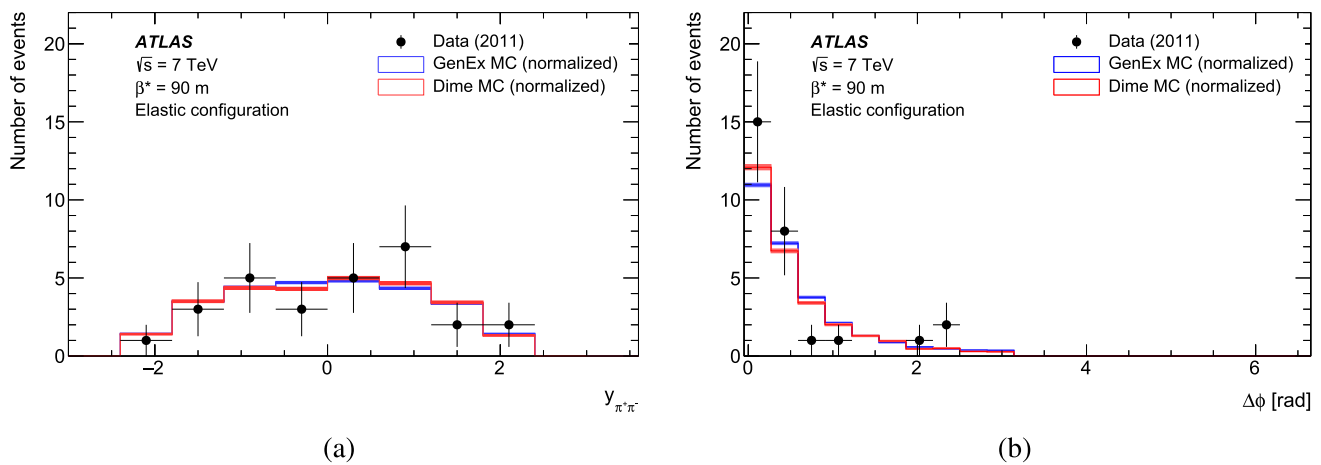


Fig. 9 Distributions of **a** pion-pair rapidity and **b** pion-pair acoplanarity for the data, GENEX MC and DIME MC simulations after applying all event selections, but without a background subtraction applied to

the data. Each of the MC samples is normalized to the data. Statistical uncertainties are shown only for the data; they are negligible for the MC predictions

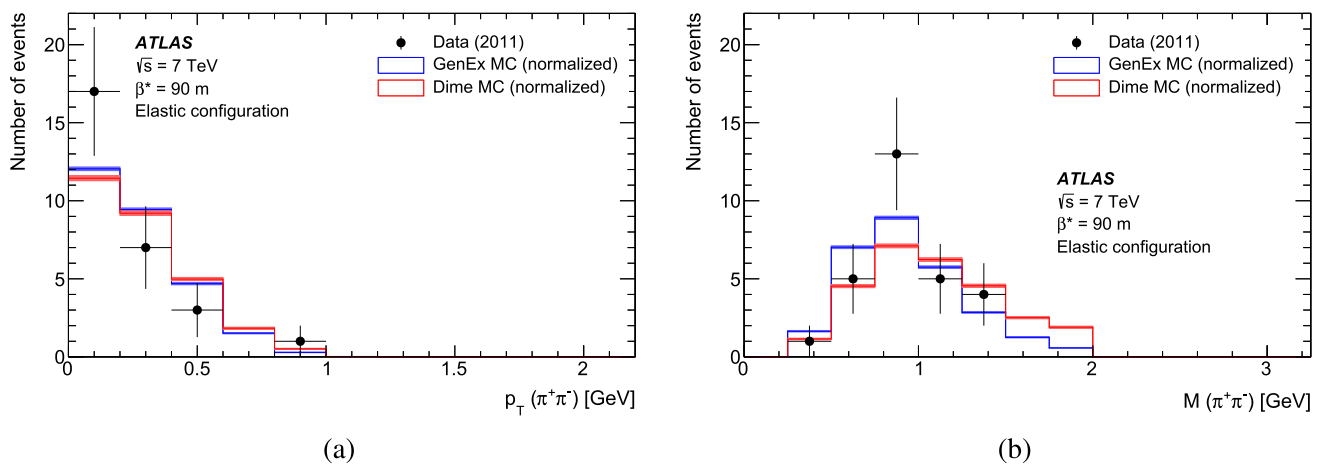


Fig. 10 Distributions of **a** pion-pair transverse momentum and **b** pion-pair invariant mass for the data, GENEX MC and DIME MC simulations after applying all event selections, but without a background subtraction

applied to the data. Each of the MC samples is normalized to the data. Statistical uncertainties are shown only for the data; they are negligible for the MC predictions

in p_x and p_y , and for the case when the signal region is increased to $5\sigma_{x,y}$. It is symmetrized.

LHC beam energy. The systematic uncertainty due to that of the nominal beam energy is based on a beam energy variation of about $\pm 0.1\%$ [41].

Thicknesses of material. An uncertainty in the amount of material in the ID is calculated by changing this by $+5\%$ and $+10\%$ in the whole ID and by $+10\%$ in the pixel detector to determine the difference between the lowest and the highest value of the corrected exclusive pion-pair cross-section [40].

MBTS Veto. The MBTS veto uncertainty determination is based on the corresponding procedure used in the measurement of the inelastic proton-proton cross-section at $\sqrt{s} = 7$ TeV [42].

Selection criteria. The uncertainty in the efficiency due to the selection criteria is determined from the fraction of lost signal. The overall uncertainty in the ALFA reconstruction efficiency is determined by varying the event selection criteria and summing the corresponding individual uncertainties in quadrature.

Correction factors. An uncertainty in the values of $f_{\text{arm}}^{s+uv, \text{conf}}$ arises from the restricted selection of data that is used to evaluate this factor in each arm. Although of statistical origin, this is treated as a systematic uncertainty.

Beam optics. This analysis uses data at a collision energy of 7 TeV and with high $\beta^* = 90$ m beam optics, referred to as the nominal optics. Based on data measurements, an adjustment is made to the current-to-field calibration offset

Table 4 Summary of the exclusive pion-pair cross-section systematic uncertainties

Source of uncertainty	Uncertainty (%)	
	Elastic	Anti-elastic
Trigger efficiency ϵ_{trig}	± 0.1	± 0.3
Background determination	± 3.5	± 3.5
Signal and background corrections:		
Beam energy	± 0.1	± 0.1
ID material	+4.8	+4.1
Veto on MBTS signal	± 1.3	± 2.0
ALFA single-track selection	± 0.9	± 0.9
ALFA reconstruction efficiency	± 0.9	± 0.8
ALFA geometry selection	± 0.5	± 0.5
Optics	± 1.1	± 1.0
Overall systematic uncertainty	+6.4	+6.0
	-4.2	-4.4
Statistical uncertainty	± 21.2	± 61.6
Theoretical modelling	± 2.8	± 8.0
Luminosity	± 1.2	± 1.2

between the Q1Q3 and Q2 quadrupole magnets to derive the so-called effective optics [9]. Studies related to both optics are performed: the effective and the nominal optics are used in MC simulation to calculate all the corrections applied in reconstructing the data. The nominal optics is used as the baseline; the difference in the cross-section values is used to determine the systematic uncertainties.

Modelling. The analysis of the data uses the generator GENEX as the baseline for modelling the signal sample. The full analysis is repeated using the generator DIME, and the difference between the resulting cross-sections is taken as an

Table 5 Exclusive pion-pair cross-section within the defined fiducial region for elastic and anti-elastic configurations, for the measurement and MC simulations. The statistical uncertainties of the MC simulations are negligible. The GENEX predictions have been multiplied by an absorptive correction factor of 0.22 suggested by the author of the generator

Exclusive $\pi^+\pi^-$ cross-section [μb]	
Elastic configuration	
Measurement	4.8 ± 1.0 (stat) $^{+0.3}_{-0.2}$ (syst) ± 0.1 (lumi) ± 0.1 (model)
GENEX $\times 0.22$ (absorptive correction)	1.5
DIME	1.6
Anti-elastic configuration	
Measurement	9 ± 6 (stat) $^{+1}_{-1}$ (syst) ± 1 (lumi) ± 1 (model)
GENEX $\times 0.22$ (absorptive correction)	2
DIME	3

uncertainty due to the modelling and is applied symmetrically.

6 Results and discussion

The cross-section for exclusive pion pair production is measured for two non-overlapping configurations, elastic and anti-elastic. The fiducial region is defined in Sect. 5.1.1 and the results are presented in Table 5.

There are 28 candidate signal events in the elastic configuration and 3 in the anti-elastic configuration (see Table 2). These include an estimated 2.9 background events in the elastic configuration ($\approx 10\%$) and 0.2 background events ($\approx 6\%$) in the anti-elastic configuration.

The results may be compared with cross-sections provided by MC generators using the same fiducial region definition: $1.5 \mu\text{b}$ (elastic configuration) and $2 \mu\text{b}$ (anti-elastic configuration) in the case of GENEX (these have been multiplied by an absorptive correction, abs. corr.), and $1.6 \mu\text{b}$ (elastic configuration) and $3 \mu\text{b}$ (anti-elastic configuration) in the case of DIME. The absorptive correction [25] applied here to GENEX covers possible rescatterings of the particles entering the process and complicates the simple picture in Fig. 1. The value used of 0.22 was communicated by its author; the correction is not included in GENEX itself and is, in general, kinematics and model dependent. It is not used in the experimental analysis, since the MC distributions are normalized to data, but only in the present comparison with the results. The measured anti-elastic cross-section has a large statistical uncertainty, and is not statistically different from zero, which prevents strong conclusions from being drawn.

7 Conclusion

A first measurement of the purely exclusive pion-pair cross-section at the LHC is presented, using $80 \mu\text{b}^{-1}$ of $\sqrt{s} = 7 \text{ TeV}$ low-luminosity pp collision data collected by the ATLAS detector. The limited statistical precision obtained excludes the present possibility of tuning or excluding any of the existing physical models for the process, but the two models that are employed here, GENEX and DIME, evaluated with the parameters provided by their authors, provide preliminary theoretical estimates. The use of the forward ALFA detectors distinguishes the present measurement from others performed at comparable energies, since both outgoing protons have been measured directly, and used to suppress contamination from beam remnants. This measurement demonstrates the potential to measure exclusive diffractive hadronic processes using forward sub-detectors in combination with the ATLAS central detector.

Acknowledgements We thank CERN for the very successful operation of the LHC, as well as the support staff from our institutions without whom ATLAS could not be operated efficiently. We acknowledge the support of ANPCyT, Argentina; YerPhI, Armenia; ARC, Australia; BMWFW and FWF, Austria; ANAS, Azerbaijan; CNPq and FAPESP, Brazil; NSERC, NRC and CFI, Canada; CERN; ANID, Chile; CAS, MOST and NSFC, China; Minciencias, Colombia; MEYS CR, Czech Republic; DNRF and DNSRC, Denmark; IN2P3-CNRS and CEA-DRF/IRFU, France; SRNSFG, Georgia; BMBF, HGF and MPG, Germany; GSRI, Greece; RGC and Hong Kong SAR, China; ISF and Benozziyo Center, Israel; INFN, Italy; MEXT and JSPS, Japan; CNRST, Morocco; NWO, Netherlands; RCN, Norway; MEiN, Poland; FCT, Portugal; MNE/IFA, Romania; MESTD, Serbia; MSSR, Slovakia; ARRS and MIZŠ, Slovenia; DSI/NRF, South Africa; MICINN, Spain; SRC and Wallenberg Foundation, Sweden; SERI, SNSF and Cantons of Bern and Geneva, Switzerland; MOST, Taiwan; TENMAK, Turkey; STFC, United Kingdom; DOE and NSF, USA. In addition, individual groups and members have received support from BCKDF, CANARIE, Compute Canada and CRC, Canada; PRIMUS 21/SCI/017 and UNCE SCI/013, Czech Republic; COST, ERC, ERDF, Horizon 2020 and Marie Skłodowska-Curie Actions, European Union; Investissements d’Avenir Labex, Investissements d’Avenir IDEX and ANR, France; DFG and AvH Foundation, Germany; Herakleitos, Thales and Aristeia programmes co-financed by EU-ESF and the Greek NSRF, Greece; BSF-NSF and MINERVA, Israel; Norwegian Financial Mechanism 2014–2021, Norway; NCN and NAWA, Poland; La Caixa Banking Foundation, CERCA Programme Generalitat de Catalunya and PROMETEO and GenT Programmes Generalitat Valenciana, Spain; Göran Gustafssons Stiftelse, Sweden; The Royal Society and Leverhulme Trust, UK. The crucial computing support from all WLCG partners is acknowledged gratefully, in particular from CERN, the ATLAS Tier-1 facilities at TRIUMF (Canada), NDGF (Denmark, Norway, Sweden), CC-IN2P3 (France), KIT/GridKA (Germany), INFN-CNAF (Italy), NL-T1 (Netherlands), PIC (Spain), ASGC (Taiwan), RAL (UK) and BNL (USA), the Tier-2 facilities worldwide and large non-WLCG resource providers. Major contributors of computing resources are listed in Ref. [43].

Data Availability Statement This manuscript has no associated data or the data will not be deposited. [Authors’ comment: “All ATLAS scientific output is published in journals, and preliminary results are made available in Conference Notes. All are openly available, without restriction on use by external parties beyond copyright law and the standard conditions agreed by CERN. Data associated with journal publications are also made available: tables and data from plots (e.g. cross section values, likelihood profiles, selection efficiencies, cross section limits, ...) are stored in appropriate repositories such as HEPDATA (<https://www.hepdata.net/>). ATLAS also strives to make additional material related to the paper available that allows a reinterpretation of the data in the context of new theoretical models. For example, an extended encapsulation of the analysis is often provided for measurements in the framework of RIVET (<http://rivet.hepforge.org/>).” This information is taken from the ATLAS Data Access Policy, which is a public document that can be downloaded from <http://opendata.cern.ch/record/413> [opendata.cern.ch]. The data for this publication will be available at: <https://doi.org/10.17182/hepdata.131222>].

Open Access This article is licensed under a Creative Commons Attribution 4.0 International License, which permits use, sharing, adaptation, distribution and reproduction in any medium or format, as long as you give appropriate credit to the original author(s) and the source, provide a link to the Creative Commons licence, and indicate if changes were made. The images or other third party material in this article are included in the article’s Creative Commons licence, unless indicated otherwise in a credit line to the material. If material is not included in the article’s Creative Commons licence and your intended use is not permitted by statutory regulation or exceeds the permit-

ted use, you will need to obtain permission directly from the copyright holder. To view a copy of this licence, visit <http://creativecommons.org/licenses/by/4.0/>.

Funded by SCOAP³. SCOAP³ supports the goals of the International Year of Basic Sciences for Sustainable Development.

References

1. Particle Data Group, Review of Particle Physics, PTEP 2020, 083C01 (2020). <https://doi.org/10.1093/ptep/ptaa104>
2. R.J. Eden, Regge poles and elementary particles. Rep. Prog. Phys. **34**, 995 (1971). <https://doi.org/10.1088/0034-4885/34/3/304>
3. O.C. Jacob, L.S. Kisslinger, Applicability of asymptotic QCD for exclusive processes. Phys. Rev. Lett. **56**, 225 (1986). <https://doi.org/10.1103/PhysRevLett.56.225>
4. V. Gribov, Possible asymptotic behavior of elastic scattering. ZhETF **41**, 667 (1961)
5. G.F. Chew, S.C. Frautschi, Principle of equivalence for all strongly interacting particles within the S-Matrix framework. Phys. Rev. Lett. **7**, 394 (1961). <https://doi.org/10.1103/PhysRevLett.7.394>
6. O. Nachtmann, Pomeron Physics and QCD. New Trends Hera Phys. **2003**, 253 (2004). https://doi.org/10.1142/9789812702722_0023
7. ATLAS Collaboration, The ATLAS Experiment at the CERN Large Hadron Collider. JINST **3**, S08003 (2008). <https://doi.org/10.1088/1748-0221/3/08/S08003>
8. S.A. Khalek et al., The ALFA Roman Pot detectors of ATLAS. JINST **11**, P11013 (2016). <https://doi.org/10.1088/1748-0221/11/11/p11013>. arXiv:1609.00249 [physics.ins-det]
9. ATLAS Collaboration, Measurement of the total cross section from elastic scattering in pp collisions at $\sqrt{s} = 7$ TeV with the ATLAS detector. Nucl. Phys. B **889**, 486 (2014). <https://doi.org/10.1016/j.nuclphysb.2014.10.019>. arXiv:1408.5778 [hep-ex]
10. A. Breakstone et al., Inclusive Pomeron–Pomeron interactions at the CERN ISR. Z. Phys. C **42**, 387 (1989). <https://doi.org/10.1007/BF01548444>. (ISSN:1431-5858)
11. A. Breakstone et al., The reaction Pomeron–Pomeron $\rightarrow \pi^+ \pi^-$ and an unusual production mechanism for the f₂ (1270). Z. Phys. C **48**, 569 (1990). <https://doi.org/10.1007/BF01614690>
12. WA91 Collaboration, A further study of the centrally produced $\pi^+ \pi^-$ and $\pi^+ \pi^- \pi^+ \pi^-$ channels in pp interactions at 300 GeV/c and 450 GeV/c. Phys. Lett. B **353**, 589 (1995). [https://doi.org/10.1016/0370-2693\(95\)00629-Y](https://doi.org/10.1016/0370-2693(95)00629-Y)
13. STAR Collaboration, Measurement of the central exclusive production of charged particle pairs in proton–proton collisions at $\sqrt{s} = 200$ GeV with the STAR detector at RHIC. JHEP **7**, 178 (2020). [https://doi.org/10.1007/JHEP07\(2020\)178](https://doi.org/10.1007/JHEP07(2020)178). arXiv:2004.11078 [hep-ex]
14. CMS Collaboration, Exclusive and semi-exclusive $\pi^+ \pi^-$ production in proton-proton collisions at $\sqrt{s} = 7$ TeV (2017). arXiv:1706.08310 [hep-ex]
15. CMS Collaboration, Study of central exclusive production in proton-proton collisions at $\sqrt{s} = 5.02$ and 13 TeV. Eur. Phys. J. C **80**, 718 (2020). <https://doi.org/10.1140/epjc/s10052-020-8166-5> (ISSN:1434-6052). arXiv:2003.02811 [hep-ex]
16. R.A. Ryutin, Central exclusive diffractive production of two-pion continuum at hadron colliders. Eur. Phys. J. C **79**, 981 (2019). <https://doi.org/10.1140/epjc/s10052-019-7497-6> (ISSN: 1434-6052). arXiv:1910.06683 [hep-ph]
17. J.R. Pelaez, A. Rodas, J. Ruiz de Elvira, Global parameterization of $\pi\pi$ scattering up to 2 GeV. Eur. Phys. J. C **79**, 1008 (2019). <https://doi.org/10.1140/epjc/s10052-019-7509-6> (ISSN: 1434-6052)
18. A.A. Godizov, The ground state of the Pomeron and its decays to light mesons and photons. Eur. Phys. J. C **76**, 361

- (2016). <https://doi.org/10.1140/epjc/s10052-016-4229-z> (ISSN: 1434-6052). [arXiv:1604.01689](https://arxiv.org/abs/1604.01689) [hep-ph]
19. P. Lebiedowicz, O. Nachtmann, A. Szczurek, Central exclusive diffractive production of $\pi^+\pi^-$ continuum, scalar and tensor resonances in pp and $p\bar{p}$ scattering within tensor pomeron approach. *Phys. Rev. D* **93**, 054015 (2016). <https://doi.org/10.1103/PhysRevD.93.054015>. [arXiv:1601.04537](https://arxiv.org/abs/1601.04537) [hep-ph]
 20. P. Lebiedowicz, O. Nachtmann, A. Szczurek, ρ^0 and Drell-Soding contributions to central exclusive production of $\pi^+\pi^-$ pairs in proton-proton collisions at high energies. *Phys. Rev. D* **91**, 074023 (2015). <https://doi.org/10.1103/PhysRevD.91.074023>. [arXiv:1612.06294](https://arxiv.org/abs/1612.06294) [hep-ph]
 21. A. Bolz et al., Photoproduction of $\pi^+\pi^-$: pairs in a model with tensor-pomeron and vector-odderon exchange. *JHEP* **01**, 151 (2015). [https://doi.org/10.1007/jhep01\(2015\)151](https://doi.org/10.1007/jhep01(2015)151) (ISSN: 1029-8479). [arXiv:1409.8483](https://arxiv.org/abs/1409.8483) [hep-ph]
 22. R. Ryutin, Visualizations of exclusive central diffraction. *Eur. Phys. J. C* **74**, 3162 (2014). <https://doi.org/10.1140/epjc/s10052-014-3162-2>. [arXiv:1404.7678](https://arxiv.org/abs/1404.7678) [hep-ph]
 23. P. Lebiedowicz, *Exclusive Reactions with Light Mesons: From Low to High Energies, Thesis* (The Henryk Niewodniczanski Institute of Nuclear Physics, Polish Academy of Sciences, 2014)
 24. P. Lebiedowicz, A. Szczurek, Exclusive $pp \rightarrow pp\pi^+\pi^-$ reaction: from the threshold to LHC. *Phys. Rev. D* **81**, 036003 (2010). <https://doi.org/10.1103/PhysRevD.81.036003>. [arXiv:0912.0190](https://arxiv.org/abs/0912.0190) [hep-ph]
 25. L.A. Harland-Lang, V.A. Khoze, M.G. Ryskin, Modelling exclusive meson pair production at hadron colliders. *Eur. Phys. J. C* **74**, 2848 (2014). <https://doi.org/10.1140/epjc/s10052-014-2848-9>. [arXiv:1312.4553](https://arxiv.org/abs/1312.4553) [hep-ph]
 26. M.G. Albrow, T.D. Coughlin, J.R. Forshaw, Central exclusive particle production at high energy hadron colliders. *Prog. Part. Nucl. Phys.* **65**, 149 (2010). <https://doi.org/10.1016/j.pnpnp.2010.06.001>. [arXiv:1006.1289](https://arxiv.org/abs/1006.1289) [hep-ph]
 27. ATLAS Collaboration, ATLAS inner detector: Technical Design Report, 1, tech. rep., CERN-LHCC-97-016; ATLAS-TDR-4 (1997)
 28. R. Kwee, Minimum Bias Triggers at ATLAS, LHC (2008). [arXiv:0812.0613](https://arxiv.org/abs/0812.0613) [hep-ex]
 29. ATLAS Collaboration, The ATLAS Collaboration Software and Firmware, ATL-SOFT-PUB-2021-001 (2021)
 30. R.A. Kycia, J. Chwastowski, R. Staszewski, J. Turnau, GenEx: a simple generator structure for exclusive processes in high energy collisions. *Commun. Comput. Phys.* **24**, 860 (2018). <https://doi.org/10.4208/cicp.OA-2017-0105> (ISSN: 1991-7120)
 31. R.A. Ryutin, ExDiff Monte Carlo generator for Exclusive Diffraction. Version 2.0. Physics and Manual (2018). [arXiv:1805.08591](https://arxiv.org/abs/1805.08591) [hep-ph]
 32. L.A. Harland-Lang, V.A. Khoze, M.G. Ryskin, Exclusive physics at the LHC with SuperChic 2. *Eur. Phys. J. C* **76**, 9 (2016). <https://doi.org/10.1140/epjc/s10052-015-3832-8> (ISSN: 1434-6052). [arXiv:1508.02718](https://arxiv.org/abs/1508.02718) [hep-ph]
 33. V.A. Khoze, A.D. Martin, M.G. Ryskin, Multiple interactions and rapidity gap survival. *J. Phys. G* **45**, 053002 (2018). <https://doi.org/10.1088/1361-6471/aab1bf>. [arXiv:1710.11505](https://arxiv.org/abs/1710.11505) [hep-ph]
 34. V.A. Khoze, A.D. Martin, M.G. Ryskin, Diffraction at the LHC. *Eur. Phys. J. C* **73** (2013). <https://doi.org/10.1140/epjc/s10052-013-2503-x> (ISSN: 1434-6052). [arXiv:1306.2149](https://arxiv.org/abs/1306.2149) [hep-ph]
 35. T. Sjöstrand, S. Mrenna, P. Skands, A brief introduction to PYTHIA 8.1. *Comput. Phys. Commun.* **178**, 852 (2008). <https://doi.org/10.1016/j.cpc.2008.01.036> (ISSN: 0010-4655). [arXiv:0710.3820](https://arxiv.org/abs/0710.3820) [hep-ph]
 36. ATLAS Collaboration, Further ATLAS tunes of Pythia 6 and Pythia 8, ATL-PHYS-PUB-2011-014 (2011)
 37. G. Watt, R.S. Thorne, Study of Monte Carlo approach to experimental uncertainty propagation with MSTW 2008 PDFs. *JHEP* **052** (2012). [https://doi.org/10.1007/jhep08\(2012\)052](https://doi.org/10.1007/jhep08(2012)052). [arXiv:1205.4024](https://arxiv.org/abs/1205.4024) [hep-ph]
 38. S. Agostinelli et al., GEANT4—a simulation toolkit. *Nucl. Instrum. Methods A* **506**, 250 (2003). [https://doi.org/10.1016/S0168-9002\(03\)01368-8](https://doi.org/10.1016/S0168-9002(03)01368-8)
 39. ATLAS Collaboration, The ATLAS Simulation Infrastructure. *Eur. Phys. J. C* **70**, 823 (2010). <https://doi.org/10.1140/epjc/s10052-010-1429-9>. [arXiv:1005.4568](https://arxiv.org/abs/1005.4568) [physics.ins-det]
 40. ATLAS Collaboration, Charged-particle multiplicities in pp interactions measured with the ATLAS detector at the LHC. *New J. Phys.* **13**, 053033 (2011). <https://doi.org/10.1088/1367-2630/13/5/053033>. [arXiv:1012.5104](https://arxiv.org/abs/1012.5104) [hep-ex]
 41. J. Wenninger, Energy Calibration of the LHC Beams at 4 TeV, tech. rep. CERN-ATS-2013-040, CERN (2013)
 42. ATLAS Collaboration, Measurement of the inelastic proton–proton cross-section at $\sqrt{s} = 7$ TeV with the ATLAS detector. *Nat. Commun.* **2**, 463 (2011). <https://doi.org/10.1038/ncomms1472>. [arXiv:1104.0326](https://arxiv.org/abs/1104.0326) [hep-ex]
 43. ATLAS Collaboration, ATLAS Computing Acknowledgements, ATL-SOFT-PUB-2021-003 (2021)

ATLAS Collaboration*

G. Aad¹⁰¹, B. Abbott¹¹⁹, D. C. Abbott¹⁰², K. Abeling⁵⁵, S. H. Abidi²⁹, A. Abouhorma^{35e}, H. Abramowicz¹⁵⁰, H. Abreu¹⁴⁹, Y. Abulaiti¹¹⁶, A. C. Abusleme Hoffman^{136a}, B. S. Acharya^{68a,68b,p}, B. Achkar⁵⁵, C. Adam Bourdarios⁴, L. Adamczyk^{84a}, L. Adamek¹⁵⁴, S. V. Addepalli²⁶, J. Adelman¹¹⁴, A. Adiguzel^{21c}, S. Adorni⁵⁶, T. Auyeub¹³³, A. A. Affolder¹³⁵, Y. Afik³⁶, M. N. Agaras¹³, J. Agarwala^{72a,72b}, A. Aggarwal⁹⁹, C. Agheorghiesei^{27c}, J. A. Aguilar-Saavedra^{129f}, A. Ahmad³⁶, F. Ahmadov^{38,x}, W. S. Ahmed¹⁰³, S. Ahuja⁹⁴, X. Ai⁴⁸, G. Aielli^{75a,75b}, I. Aizenberg¹⁶⁸, M. Akbiyik⁹⁹, T. P. A. Åkesson⁹⁷, A. V. Akimov³⁷, K. Al Khoury⁴¹, G. L. Alberghi^{23b}, J. Albert¹⁶⁴, P. Albicocco⁵³, S. Alderweireldt⁵², M. Aleksa³⁶, I. N. Aleksandrov³⁸, C. Alexa^{27b}, T. Alexopoulos¹⁰, A. Alfonsi¹¹³, F. Alfonsi^{23b}, M. Alhroob¹¹⁹, B. Ali¹³¹, S. Ali¹⁴⁷, M. Aliev³⁷, G. Alimonti^{70a}, W. Alkakh⁵⁵, C. Allaire⁶⁶, B. M. M. Allbrooke¹⁴⁵, P. P. Allport²⁰, A. Aloisio^{71a,71b}, F. Alonso⁸⁹, C. Alpigiani¹³⁷, E. Alunno Camelia^{75a,75b}, M. Alvarez Estevez⁹⁸, M. G. Alvigi^{71a,71b}, M. Aly¹⁰⁰, Y. Amaral Coutinho^{81b}, A. Ambler¹⁰³, C. Amelung³⁶, M. Ameri¹, C. G. Ames¹⁰⁸, D. Amidei¹⁰⁵, S. P. Amor Dos Santos^{129a}, S. Amoroso⁴⁸, K. R. Amos¹⁶², V. Ananiev¹²⁴, C. Anastopoulos¹³⁸, T. Andeen¹¹, J. K. Anders¹⁹, S. Y. Andreev^{47a,47b}, A. Andreazza^{70a,70b}, S. Angelidakis⁹, A. Angerami^{41,z}, A. V. Anisenkov³⁷, A. Annovi^{73a}, C. Antel⁵⁶, M. T. Anthony¹³⁸, E. Antipov¹²⁰, M. Antonelli⁵³, D. J. A. Antrim^{17a}, F. Anulli^{74a}, M. Aoki⁸², T. Aoki¹⁵², J. A. Aparisi Pozo¹⁶², M. A. Aparo¹⁴⁵, L. Aperio Bella⁴⁸, C. Appelt¹⁸, N. Aranzabal³⁶, V. Araujo Ferraz^{81a}, C. Arcangeletti⁵³, A. T. H. Arce⁵¹, E. Arena⁹¹, J.-F. Arguin¹⁰⁷, S. Argyropoulos⁵⁴, J.-H. Arling⁴⁸, A. J. Armbruster³⁶, O. Arnaez¹⁵⁴, H. Arnold¹¹³, Z. P. Arrubarrena Tame¹⁰⁸, G. Artoni^{74a,74b}, H. Asada¹¹⁰, K. Asai¹¹⁷, S. Asai¹⁵², N. A. Asbah⁶¹, J. Assahsah^{35d}, K. Assamagan²⁹, R. Astalos^{28a}, R. J. Atkin^{33a}, M. Atkinson¹⁶¹, N. B. Atlay¹⁸, H. Atmani^{62b}, P. A. Atlasiddha¹⁰⁵, K. Augsten¹³¹, S. Auricchio^{71a,71b}, A. D. Aurioi²⁰, V. A. Austrup¹⁷⁰, G. Avner¹⁴⁹, G. Avolio³⁶, K. Axiotis⁵⁶, M. K. Ayoub^{14c}, G. Azuelos^{107,ac}, D. Babal^{28a}, H. Bachacou¹³⁴, K. Bachas^{151,r}, A. Bachiu³⁴, F. Backman^{47a,47b}, A. Badea⁶¹, P. Bagnaia^{74a,74b}, M. Bahmani¹⁸, A. J. Bailey¹⁶², V. R. Bailey¹⁶¹, J. T. Baines¹³³, C. Bakalis¹⁰, O. K. Baker¹⁷¹, P. J. Bakker¹¹³, E. Bakos¹⁵, D. Bakshi Gupta⁸, S. Balaji¹⁴⁶, R. Balasubramanian¹¹³, E. M. Baldin³⁷, P. Balek¹³², E. Ballabene^{70a,70b}, F. Balli¹³⁴, L. M. Baltes^{63a}, W. K. Balunas³², J. Balz⁹⁹, E. Banas⁸⁵, M. Bandieramonte¹²⁸, A. Bandyopadhyay²⁴, S. Bansal²⁴, L. Barak¹⁵⁰, E. L. Barberio¹⁰⁴, D. Barberis^{57a,57b}, M. Barbero¹⁰¹, G. Barbour⁹⁵, K. N. Barends^{33a}, T. Barillari¹⁰⁹, M.-S. Barisits³⁶, T. Barklow¹⁴², R. M. Barnett^{17a}, P. Baron¹²¹, D. A. Baron Moreno¹⁰⁰, A. Baroncelli^{62a}, G. Barone²⁹, A. J. Barr¹²⁵, L. Barranco Navarro^{47a,47b}, F. Barreiro⁹⁸, J. Barreiro Guimarães da Costa^{14a}, U. Barron¹⁵⁰, M. G. Barros Teixeira^{129a}, S. Barsov³⁷, F. Bartels^{63a}, R. Bartoldus¹⁴², A. E. Barton⁹⁰, P. Bartos^{28a}, A. Basalaeu⁴⁸, A. Basan⁹⁹, M. Baselga⁴⁹, I. Bashta^{76a,76b}, A. Bassalat^{66,b}, M. J. Basso¹⁵⁴, C. R. Basson¹⁰⁰, R. L. Bates⁵⁹, S. Batlamous^{35c}, J. R. Batley³², B. Batool¹⁴⁰, M. Battaglia¹³⁵, D. Battulga¹⁸, M. Bause^{74a,74b}, P. Bauer²⁴, A. Bayirli^{21a}, J. B. Beacham⁵¹, T. Beau¹²⁶, P. H. Beauchemin¹⁵⁷, F. Becherer⁵⁴, P. Bechtel²⁴, H. P. Beck^{19,q}, K. Becker¹⁶⁶, A. J. Beddall^{21d}, V. A. Bednyakov³⁸, C. P. Bee¹⁴⁴, L. J. Beamster¹⁵, T. A. Beermann³⁶, M. Begalli^{81d}, M. Begel²⁹, A. Behera¹⁴⁴, J. K. Behr⁴⁸, C. Beirao Da Cruz E Silva³⁶, J. F. Beirer^{36,55}, F. Beisiegel²⁴, M. Belfkir¹⁵⁸, G. Bella¹⁵⁰, L. Bellagamba^{23b}, A. Bellerive³⁴, P. Bellos²⁰, K. Beloborodov³⁷, K. Belotskiy³⁷, N. L. Belyaev³⁷, D. Bencheikroun^{35a}, F. Bendebba^{35a}, Y. Benhammou¹⁵⁰, D. P. Benjamin²⁹, M. Benoit²⁹, J. R. Bensinger²⁶, S. Bentvelsen¹¹³, L. Beresford³⁶, M. Beretta⁵³, D. Berge¹⁸, E. Bergeas Kuutmann¹⁶⁰, N. Berger⁴, B. Bergmann¹³¹, J. Beringer^{17a}, S. Berlendis⁷, G. Bernardi⁵, C. Bernius¹⁴², F. U. Bernlochner²⁴, T. Berry⁹⁴, P. Berta¹³², A. Berthold⁵⁰, I. A. Bertram⁹⁰, S. Bethke¹⁰⁹, A. Betti^{74a,74b}, A. J. Bevan⁹³, M. Bhamjee^{33c}, S. Bhatta¹⁴⁴, D. S. Bhattacharya¹⁶⁵, P. Bhattarai²⁶, V. S. Bhopatkar¹²⁰, R. Bi^{29,af}, R. M. Bianchi¹²⁸, O. Biebel¹⁰⁸, R. Bielski¹²², M. Biglietti^{76a}, T. R. V. Billoud¹³¹, M. Bindi⁵⁵, A. Bingul^{21b}, C. Bini^{74a,74b}, S. Biondi^{23a,23b}, A. Biondini⁹¹, C. J. Birch-sykes¹⁰⁰, G. A. Bird^{20,133}, M. Birman¹⁶⁸, T. Bisanz³⁶, E. Bisceglie^{43a,43b}, D. Biswas^{169,1}, A. Bitadze¹⁰⁰, K. Björke¹²⁴, I. Bloch⁴⁸, C. Blocker²⁶, A. Blue⁵⁹, U. Blumenschein⁹³, J. Blumenthal⁹⁹, G. J. Bobbink¹¹³, V. S. Bobrovnikov³⁷, M. Boehler⁵⁴, D. Bogavac³⁶, A. G. Bogdanchikov³⁷, C. Boehm^{47a}, V. Boisvert⁹⁴, P. Bokan⁴⁸, T. Bold^{84a}, M. Bomben⁵, M. Bona⁹³, M. Boonekamp¹³⁴, C. D. Booth⁹⁴, A. G. Borbély⁵⁹, H. M. Borecka-Bielska¹⁰⁷, L. S. Borgna⁹⁵, G. Borissov⁹⁰, D. Bortoletto¹²⁵, D. Boscherini^{23b}, M. Bosman¹³, J. D. Bossio Sola³⁶, K. Bouaouda^{35a}, N. Bouchhar¹⁶², J. Boudreau¹²⁸, E. V. Bouhova-Thacker⁹⁰, D. Boumediene⁴⁰, R. Bouquet⁵, A. Boveia¹¹⁸, J. Boyd³⁶, D. Boye²⁹, I. R. Boyko³⁸, J. Bracinik²⁰, N. Brahimi^{62d}, G. Brandt¹⁷⁰, O. Brandt³², F. Braren⁴⁸, B. Brau¹⁰²,

J. E. Brau¹²², K. Brendlinger⁴⁸, R. Brenner¹⁶⁸, L. Brenner¹¹³, R. Brenner¹⁶⁰, S. Bressler¹⁶⁸, B. Brickwedde⁹⁹, D. Britton⁵⁹, D. Britzger¹⁰⁹, I. Brock²⁴, G. Brooijmans⁴¹, W. K. Brooks^{136f}, E. Brost²⁹, T. L. Bruckler¹²⁵, P. A. Bruckman de Renstrom⁸⁵, B. Brüers⁴⁸, D. Bruncko^{28b,*}, A. Bruni^{23b}, G. Bruni^{23b}, M. Bruschi^{23b}, N. Bruscinò^{74a,74b}, L. Bryngemark¹⁴², T. Buanes¹⁶, Q. Buat¹³⁷, P. Buchholz¹⁴⁰, A. G. Buckley⁵⁹, I. A. Budagov^{38,*}, M. K. Bugge¹²⁴, O. Bulekov³⁷, B. A. Bullard⁶¹, S. Burdin⁹¹, C. D. Burgard⁴⁸, A. M. Burger⁴⁰, B. Burghgrave⁸, J. T. P. Burr³², C. D. Burton¹¹, J. C. Burzynski¹⁴¹, E. L. Busch⁴¹, V. Büscher⁹⁹, P. J. Bussey⁵⁹, J. M. Butler²⁵, C. M. Buttar⁵⁹, J. M. Butterworth⁹⁵, W. Buttinger¹³³, C. J. Buxo Vazquez¹⁰⁶, A. R. Buzykaev³⁷, G. Cabras^{23b}, S. Cabrera Urbán¹⁶², D. Caforio⁵⁸, H. Cai¹²⁸, Y. Cai^{14a,14d}, V. M. M. Cairo³⁶, O. Cakir^{3a}, N. Calace³⁶, P. Calafiura^{17a}, G. Calderini¹²⁶, P. Calfayan⁶⁷, G. Callea⁵⁹, L. P. Caloba^{81b}, D. Calvet⁴⁰, S. Calvet⁴⁰, T. P. Calvet¹⁰¹, M. Calvetti^{73a,73b}, R. Camacho Toro¹²⁶, S. Camarda³⁶, D. Camarero Munoz²⁶, P. Camarri^{75a,75b}, M. T. Camerlingo^{76a,76b}, D. Cameron¹²⁴, C. Camincher¹⁶⁴, M. Campanelli⁹⁵, A. Camplani⁴², V. Canale^{71a,71b}, A. Canesse¹⁰³, M. Cano Bret⁷⁹, J. Cantero¹⁶², Y. Cao¹⁶¹, F. Capocasa²⁶, M. Capua^{43a,43b}, A. Carbone^{70a,70b}, R. Cardarelli^{75a}, J. C. J. Cardenas⁸, F. Cardillo¹⁶², T. Carli³⁶, G. Carlino^{71a}, J. I. Carlotto¹³, B. T. Carlson^{128,s}, E. M. Carlson^{155a,164}, L. Carminati^{70a,70b}, M. Carnesale^{74a,74b}, S. Caron¹¹², E. Carquin^{136f}, S. Carrá^{70a,70b}, G. Carratta^{23a,23b}, F. Carrio Argos^{33g}, J. W. S. Carter¹⁵⁴, T. M. Carter⁵², M. P. Casado^{13,i}, A. F. Casha¹⁵⁴, E. G. Castiglia¹⁷¹, F. L. Castillo^{63a}, L. Castillo Garcia¹³, V. Castillo Gimenez¹⁶², N. F. Castro^{129a,129e}, A. Catinaccio³⁶, J. R. Catmore¹²⁴, V. Cavaliere²⁹, N. Cavalli^{23a,23b}, V. Cavasinni^{73a,73b}, E. Celebi^{21a}, F. Celli¹²⁵, M. S. Centonze^{69a,69b}, K. Cerny¹²¹, A. S. Cerqueira^{81a}, A. Cerri¹⁴⁵, L. Cerrito^{75a,75b}, F. Cerutti^{17a}, A. Cervelli^{23b}, S. A. Cetin^{21d}, Z. Chadi^{35a}, D. Chakraborty¹¹⁴, M. Chala^{129f}, J. Chan¹⁶⁹, W. Y. Chan¹⁵², J. D. Chapman³², B. Chargeishvili^{148b}, D. G. Charlton²⁰, T. P. Charman⁹³, M. Chatterjee¹⁹, S. Chekanov⁶, S. V. Chekulaev^{155a}, G. A. Chelkov^{38,a}, A. Chen¹⁰⁵, B. Chen¹⁵⁰, B. Chen¹⁶⁴, C. Chen^{62a}, H. Chen^{14c}, H. Chen²⁹, J. Chen^{62c}, J. Chen²⁶, S. Chen¹⁵², S. J. Chen^{14c}, X. Chen^{62c}, X. Chen^{14b,ab}, Y. Chen^{62a}, C. L. Cheng¹⁶⁹, H. C. Cheng^{64a}, S. Cheong¹⁴², A. Cheplakov³⁸, E. Cheremushkina⁴⁸, E. Cherepanova¹¹³, R. Cherkaoui El Moursli^{35e}, E. Cheu⁷, K. Cheung⁶⁵, L. Chevalier¹³⁴, V. Chiarella⁵³, G. Chiarelli^{73a}, N. Chiedde¹⁰¹, G. Chiodini^{69a}, A. S. Chisholm²⁰, A. Chitan^{27b}, M. Chitishvili¹⁶², Y. H. Chiu¹⁶⁴, M. V. Chizhov³⁸, K. Choi¹¹, A. R. Chomont^{74a,74b}, Y. Chou¹⁰², E. Y. S. Chow¹¹³, T. Chowdhury^{33g}, L. D. Christopher^{33g}, K. L. Chu^{64a}, M. C. Chu^{64a}, X. Chu^{14a,14d}, J. Chudoba¹³⁰, J. J. Chwastowski⁸⁵, D. Cieri¹⁰⁹, K. M. Ciesla^{84a}, V. Cindro⁹², A. Ciocio^{17a}, F. Ciotto^{71a,71b}, Z. H. Citron^{168,m}, M. Citterio^{70a}, D. A. Ciubotaru^{27b}, B. M. Ciungu¹⁵⁴, A. Clark⁵⁶, P. J. Clark⁵², J. M. Clavijo Columbie⁴⁸, S. E. Clawson¹⁰⁰, C. Clement^{47a,47b}, J. Clercx⁴⁸, L. Clissa^{23a,23b}, Y. Coadou¹⁰¹, M. Cobal^{68a,68c}, A. Coccaro^{57b}, R. F. Coelho Barrue^{129a}, R. Coelho Lopes De Sa¹⁰², S. Coelli^{70a}, H. Cohen¹⁵⁰, A. E. C. Coimbra^{70a,70b}, B. Cole⁴¹, J. Collot⁶⁰, P. Conde Muñoa^{129a,129g}, M. P. Connell^{33c}, S. H. Connell^{33c}, I. A. Connelly⁵⁹, E. I. Conroy¹²⁵, F. Conventi^{71a,ad}, H. G. Cooke²⁰, A. M. Cooper-Sarkar¹²⁵, F. Cormier¹⁶³, L. D. Corpe³⁶, M. Corradi^{74a,74b}, E. E. Corrigan⁹⁷, F. Corriveau^{103,w}, A. Cortes-Gonzalez¹⁸, M. J. Costa¹⁶², F. Costanza⁴, D. Costanzo¹³⁸, B. M. Cote¹¹⁸, G. Cowan⁹⁴, J. W. Cowley³², K. Cranmer¹¹⁶, S. Crépe-Renaudin⁶⁰, F. Crescioli¹²⁶, M. Cristinziani¹⁴⁰, M. Cristoforetti^{77a,77b,d}, V. Croft¹⁵⁷, G. Crosetti^{43a,43b}, A. Cueto³⁶, T. Cuhadar Donszelmann¹⁵⁹, H. Cui^{14a,14d}, Z. Cui⁷, A. R. Cukierman¹⁴², W. R. Cunningham⁵⁹, F. Curcio^{43a,43b}, P. Czodrowski³⁶, M. M. Czurylo^{63b}, M. J. Da Cunha Sargedas De Sousa^{62a}, J. V. Da Fonseca Pinto^{81b}, C. Da Via¹⁰⁰, W. Dabrowski^{84a}, T. Dado⁴⁹, S. Dahbi^{33g}, T. Dai¹⁰⁵, C. Dallapiccola¹⁰², M. Dam⁴², G. D'amen²⁹, V. D'Amico¹⁰⁸, J. Damp⁹⁹, J. R. Dandoy¹²⁷, M. F. Daneri³⁰, M. Danninger¹⁴¹, V. Dao³⁶, G. Darbo^{57b}, S. Darmora⁶, S. J. Das²⁹, S. D'Auria^{70a,70b}, C. David^{155b}, T. Davidek¹³², D. R. Davis⁵¹, B. Davis-Purcell³⁴, I. Dawson⁹³, K. De⁸, R. De Asmundis^{71a}, M. De Beurs¹¹³, N. De Biase⁴⁸, S. De Castro^{23a,23b}, N. De Groot¹¹², P. de Jong¹¹³, H. De la Torre¹⁰⁶, A. De Maria^{14c}, A. De Salvo^{74a}, U. De Sanctis^{75a,75b}, A. De Santo¹⁴⁵, J. B. De Vivie De Regie⁶⁰, D. V. Dedovich³⁸, J. Degens¹¹³, A. M. Deiana⁴⁴, F. Del Corso^{23a,23b}, J. Del Peso⁹⁸, F. Del Rio^{63a}, F. Deliot¹³⁴, C. M. Delitzsch⁴⁹, M. Della Pietra^{71a,71b}, D. Della Volpe⁵⁶, A. Dell'Acqua³⁶, L. Dell'Asta^{70a,70b}, M. Delmastro⁴, P. A. Delsart⁶⁰, S. Demers¹⁷¹, M. Demichev³⁸, S. P. Denisov³⁷, L. D'ErAMO¹¹⁴, D. Derendarz⁸⁵, F. Derue¹²⁶, P. Dervan⁹¹, K. Desch²⁴, K. Dette¹⁵⁴, C. Deutsch²⁴, P. O. Deviveiros³⁶, F. A. Di Bello^{74a,74b}, A. Di Ciaccio^{75a,75b}, L. Di Ciaccio⁴, A. Di Domenico^{74a,74b}, C. Di Donato^{71a,71b}, A. Di Girolamo³⁶, G. Di Gregorio^{73a,73b}, A. Di Luca^{77a,77b}, B. Di Micco^{76a,76b}, R. Di Nardo^{76a,76b}, C. Diaconu¹⁰¹, F. A. Dias¹¹³, T. Dias Do Vale¹⁴¹, M. A. Diaz^{136a,136b}, F. G. Diaz Capriles²⁴, M. Didenko¹⁶², E. B. Diehl¹⁰⁵, L. Diehl⁵⁴, S. Díez Cornell⁴⁸, C. Díez Pardos¹⁴⁰

C. Dimitriadis^{24,160}, A. Dimitrievska^{17a}, W. Ding^{14b}, J. Dingfelder²⁴, I-M. Dinu^{27b}, S. J. Dittmeier^{63b}, F. Dittus³⁶, F. Djama¹⁰¹, T. Djobava^{148b}, J. I. Djuvslund¹⁶, C. Doglioni^{97,100}, J. Dolejsi¹³², Z. Dolezal¹³², M. Donadelli^{81c}, B. Dong^{62c}, J. Donini⁴⁰, A. D’Onofrio^{14c}, M. D’Onofrio⁹¹, J. Dopke¹³³, A. Doria^{71a}, M. T. Dova⁸⁹, A. T. Doyle⁵⁹, M. A. Draguet¹²⁵, E. Drechsler¹⁴¹, E. Dreyer¹⁶⁸, I. Drivas-koulouris¹⁰, A. S. Drobac¹⁵⁷, M. Drozdova⁵⁶, D. Du^{62a}, T. A. du Pree¹¹³, F. Dubinin³⁷, M. Dubovsky^{28a}, E. Duchovni¹⁶⁸, G. Duckeck¹⁰⁸, O. A. Ducu^{27b}, D. Duda¹⁰⁹, A. Dudarev³⁶, M. D’uffizi¹⁰⁰, L. Duflot⁶⁶, M. Dührssen³⁶, C. Dülsen¹⁷⁰, A. E. Dumitriu^{27b}, M. Dunford^{63a}, S. Dungs⁴⁹, K. Dunne^{47a,47b}, A. Duperrin¹⁰¹, H. Duran Yildiz^{3a}, M. Düren⁵⁸, A. Durglishvili^{148b}, B. L. Dwyer¹¹⁴, G. I. Dyckes^{17a}, M. Dyndal^{84a}, S. Dysch¹⁰⁰, B. S. Dziedzic⁸⁵, Z. O. Earnshaw¹⁴⁵, B. Eckerova^{28a}, M. G. Eggleston⁵¹, E. Egidio Purcino De Souza^{81b}, L. F. Ehrke⁵⁶, G. Eigen¹⁶, K. Einsweiler^{17a}, T. Ekelof¹⁶⁰, P. A. Ekman⁹⁷, Y. El Ghazali^{35b}, H. El Jarrari^{35e,147}, A. El Moussaouy^{35a}, V. Ellajosyula¹⁶⁰, M. Ellert¹⁶⁰, F. Ellinghaus¹⁷⁰, A. A. Elliot⁹³, N. Ellis³⁶, J. Elmsheuser²⁹, M. Elsing³⁶, D. Emelianov¹³³, A. Emerman⁴¹, Y. Enari¹⁵², I. Ene^{17a}, S. Epari¹³, J. Erdmann^{49,aa}, A. Ereditato¹⁹, P. A. Erland⁸⁵, M. Errenst¹⁷⁰, M. Escalier⁶⁶, C. Escobar¹⁶², E. Etzion¹⁵⁰, G. Evans^{129a}, H. Evans⁶⁷, M. O. Evans¹⁴⁵, A. Ezhilov³⁷, S. Ezzarqtouni^{35a}, F. Fabbri⁵⁹, L. Fabbri^{23a,23b}, G. Facini⁹⁵, V. Fadeyev¹³⁵, R. M. Fakhrtudinov³⁷, S. Falciano^{74a}, P. J. Falke²⁴, S. Falke³⁶, J. Faltova¹³², Y. Fan^{14a}, Y. Fang^{14a,14d}, G. Fanourakis⁴⁶, M. Fanti^{70a,70b}, M. Faraj^{68a,68b}, A. Farbin⁸, A. Farilla^{76a}, T. Faroouque¹⁰⁶, S. M. Farrington⁵², F. Fassi^{35c}, D. Fassouliotis⁹, M. Fauci Giannelli^{75a,75b}, W. J. Fawcett³², L. Fayard⁶⁶, P. Federicova¹³⁰, O. L. Fedin^{37,a}, G. Fedotov³⁷, M. Feickert¹⁶¹, L. Felgioni¹⁰¹, A. Fell¹³⁸, D. E. Fellers¹²², C. Feng^{62b}, M. Feng^{14b}, Z. Feng¹¹³, M. J. Fenton¹⁵⁹, A. B. Fenyuk³⁷, L. Ferencz⁴⁸, S. W. Ferguson⁴⁵, J. Ferrando⁴⁸, A. Ferrari¹⁶⁰, P. Ferrari^{112,113}, R. Ferrari^{72a}, D. Ferrere⁵⁶, C. Ferretti¹⁰⁵, F. Fiedler⁹⁹, A. Filipčić⁹², E. K. Filmer¹, F. Filthaut¹¹², M. C. N. Fiolhais^{129a,129c,c}, L. Fiorini¹⁶², F. Fischer¹⁴⁰, W. C. Fisher¹⁰⁶, T. Fitschen²⁰, I. Fleck¹⁴⁰, P. Fleischmann¹⁰⁵, T. Flick¹⁷⁰, L. Flores¹²⁷, M. Flores^{33d}, L. R. Flores Castillo^{64a}, F. M. Follega^{77a,77b}, N. Fomin¹⁶, J. H. Foo¹⁵⁴, B. C. Forland⁶⁷, A. Formica¹³⁴, A. C. Forti¹⁰⁰, E. Fortin¹⁰¹, A. W. Fortman⁶¹, M. G. Foti^{17a}, L. Fountas⁹, D. Fournier⁶⁶, H. Fox⁹⁰, P. Francavilla^{73a,73b}, S. Francescato⁶¹, M. Franchini^{23a,23b}, S. Franchino^{63a}, D. Francis³⁶, L. Franco¹¹², L. Franconi¹⁹, M. Franklin⁶¹, G. Frattari²⁶, A. C. Freegard⁹³, P. M. Freeman²⁰, W. S. Freund^{81b}, N. Fritzsche⁵⁰, A. Froch⁵⁴, D. Froidevaux³⁶, J. A. Frost¹²⁵, Y. Fu^{62a}, M. Fujimoto¹¹⁷, E. Fullana Torregrosa^{162,*}, J. Fuster¹⁶², A. Gabrielli^{23a,23b}, A. Gabrielli¹⁵⁴, P. Gadow⁴⁸, G. Gagliardi^{57a,57b}, L. G. Gagnon^{17a}, G. E. Gallardo¹²⁵, E. J. Gallas¹²⁵, B. J. Gallop¹³³, R. Gamboa Goni⁹³, K. K. Gan¹¹⁸, S. Ganguly¹⁵², J. Gao^{62a}, Y. Gao⁵², F. M. Garay Walls^{136a,136b}, B. Garcia^{29,af}, C. García¹⁶², J. E. García Navarro¹⁶², J. A. García Pascual^{14a}, M. Garcia-Sciveres^{17a}, R. W. Gardner³⁹, D. Garg⁷⁹, R. B. Garg¹⁴², S. Gargiulo⁵⁴, C. A. Garner¹⁵⁴, V. Garonne²⁹, S. J. Gasiorowski¹³⁷, P. Gaspar^{81b}, G. Gaudio^{72a}, V. Gautam¹³, P. Gauzzi^{74a,74b}, I. L. Gavrilenko³⁷, A. Gavrilyuk³⁷, C. Gay¹⁶³, G. Gaycken⁴⁸, E. N. Gaziz¹⁰, A. A. Geanta^{27b,27e}, C. M. Gee¹³⁵, J. Geisen⁹⁷, M. Geisen⁹⁹, C. Gemme^{57b}, M. H. Genest⁶⁰, S. Gentile^{74a,74b}, S. George⁹⁴, W. F. George²⁰, T. Gerialis⁴⁶, L. O. Gerlach⁵⁵, P. Gessinger-Befurt³⁶, M. Ghasemi Bostanabad¹⁶⁴, M. Ghneimat¹⁴⁰, K. Ghorbanian⁹³, A. Ghosal¹⁴⁰, A. Ghosh¹⁵⁹, A. Ghosh⁷, B. Giacobbe^{23b}, S. Giagu^{74a,74b}, N. Giangiacomi¹⁵⁴, P. Giannetti^{73a}, A. Giannini^{62a}, S. M. Gibson⁹⁴, M. Gignac¹³⁵, D. T. Gil^{84b}, A. K. Gilbert^{84a}, B. J. Gilbert⁴¹, D. Gillberg³⁴, G. Gilles¹¹³, N. E. K. Gillwald⁴⁸, L. Ginabat¹²⁶, D. M. Gingrich^{2,ac}, M. P. Giordani^{68a,68c}, P. F. Giraud¹³⁴, G. Giugliarelli^{68a,68c}, D. Giugni^{70a}, F. Giulini³⁶, I. Gkialas^{9,j}, L. K. Gladilin³⁷, C. Glasman⁹⁸, G. R. Gledhill¹²², M. Glisic¹²², I. Gnesi^{43b,f}, Y. Go^{29,af}, M. Goblirsch-Kolb²⁶, D. Godin¹⁰⁷, S. Goldfarb¹⁰⁴, T. Golling⁵⁶, M. G. D. Gololo^{33g}, D. Golubkov³⁷, J. P. Gombas¹⁰⁶, A. Gomes^{129a,129b}, G. Gomes Da Silva¹⁴⁰, A. J. Gomez Delegido¹⁶², R. Goncalves Gama⁵⁵, R. Gonçalo^{129a,129c}, G. Gonella¹²², L. Gonella²⁰, A. Gongadze³⁸, F. Gonnella²⁰, J. L. Gonski⁴¹, R. Y. González Andana⁵², S. González de la Hoz¹⁶², S. Gonzalez Fernandez¹³, R. Gonzalez Lopez⁹¹, C. Gonzalez Renteria^{17a}, R. Gonzalez Suarez¹⁶⁰, S. Gonzalez-Sevilla⁵⁶, G. R. Gonzalez-Rodriguez¹⁶², L. Goossens³⁶, N. A. Gorasia²⁰, P. A. Gorbounov³⁷, B. Gorini³⁶, E. Gorini^{69a,69b}, A. Gorišek⁹², A. T. Goshaw⁵¹, M. I. Gostkin³⁸, C. A. Gottardo³⁶, M. Gouighri^{35b}, V. Goumarre⁴⁸, A. G. Goussiou¹³⁷, N. Govender^{33c}, C. Goy⁴, I. Grabowska-Bold^{84a}, K. Graham³⁴, E. Gramstad¹²⁴, S. Grancagnolo¹⁸, M. Grandi¹⁴⁵, V. Gratchev^{37,*}, P. M. Gravila^{27f}, F. G. Gravili^{69a,69b}, H. M. Gray^{17a}, M. Greco^{69a,69b}, C. Grefe²⁴, I. M. Gregor⁴⁸, P. Grenier¹⁴², C. Grieco¹³, A. A. Grillo¹³⁵, K. Grimm^{31,n}, S. Grinstein^{13,u}, J.-F. Grivaz⁶⁶, E. Gross¹⁶⁸, J. Grosse-Knetter⁵⁵, C. Grud¹⁰⁵, A. Grummer¹¹¹, J. C. Grundy¹²⁵, L. Guan¹⁰⁵, W. Guan¹⁶⁹, C. Gubbels¹⁶³, J. G. R. Guerrero Rojas¹⁶², G. Guerrieri^{68a,68b}, F. Guescini¹⁰⁹, R. Gugel⁹⁹,

G. Pezzullo¹⁷¹, T. M. Pham¹⁶⁹, T. Pham¹⁰⁴, P. W. Phillips¹³³, M. W. Phipps¹⁶¹, G. Piacquadio¹⁴⁴, E. Pianori^{17a}, F. Piazza^{70a,70b}, R. Piegai³⁰, D. Pietreanu^{27b}, A. D. Pilkington¹⁰⁰, M. Pinamonti^{68a,68c}, J. L. Pinfold², B. C. Pinheiro Pereira^{129a}, C. Pitman Donaldson⁹⁵, D. A. Pizzi³⁴, L. Pizzimento^{75a,75b}, A. Pizzini¹¹³, M. -A. Pleier²⁹, V. Plesanovs⁵⁴, V. Pleskot¹³², E. Plotnikova³⁸, G. Poddar⁴, R. Poettgen⁹⁷, L. Poggioli¹²⁶, I. Pogrebnyak¹⁰⁶, D. Pohl²⁴, I. Pokharel⁵⁵, S. Polacek¹³², G. Polesello^{72a}, A. Poley^{141,155a}, R. Polifka¹³¹, A. Polini^{23b}, C. S. Pollard¹²⁵, Z. B. Pollock¹¹⁸, V. Polychronakos²⁹, E. Pompa Pacchi^{74a,74b}, D. Ponomarenko³⁷, L. Pontecorvo³⁶, S. Popa^{27a}, G. A. Popeneciu^{27d}, D. M. Portillo Quintero^{155a}, S. Pospisil¹³¹, P. Postolache^{27c}, K. Potamianos¹²⁵, I. N. Potrap³⁸, C. J. Potter³², H. Potti¹, T. Poulsen⁴⁸, J. Poveda¹⁶², M. E. Pozo Astigarraga³⁶, A. Prades Ibanez¹⁶², M. M. Prapa⁴⁶, J. Pretel⁵⁴, D. Price¹⁰⁰, M. Primavera^{69a}, M. A. Principe Martin⁹⁸, R. Privara¹²¹, M. L. Proffitt¹³⁷, N. Proklova¹²⁷, K. Prokofiev^{64c}, G. Proto^{75a,75b}, S. Protopopescu²⁹, J. Proudfoot⁶, M. Przybycien^{84a}, J. E. Puddefoot¹³⁸, D. Pudzha³⁷, P. Puzo⁶⁶, D. Pyatiizbyantseva³⁷, J. Qian¹⁰⁵, D. Qichen¹⁰⁰, Y. Qin¹⁰⁰, T. Qiu⁹³, A. Quadt⁵⁵, M. Queitsch-Maitland¹⁰⁰, G. Quetant⁵⁶, G. Rabanal Bolanos⁶¹, D. Rafanoharana⁵⁴, F. Ragusa^{70a,70b}, J. L. Rainbolt³⁹, J. A. Raine⁵⁶, S. Rajagopalan²⁹, E. Ramakoti³⁷, K. Ran^{48,14d}, N. P. Rapheeha^{33g}, V. Raskina¹²⁶, D. F. Rassloff^{63a}, S. Rave⁹⁹, B. Ravina⁵⁵, I. Ravinovich¹⁶⁸, M. Raymond³⁶, A. L. Read¹²⁴, N. P. Readioff¹³⁸, D. M. Rebuffi^{72a,72b}, G. Redlinger²⁹, K. Reeves⁴⁵, J. A. Reidelsturz¹⁷⁰, D. Reikher¹⁵⁰, A. Reiss⁹⁹, A. Rej¹⁴⁰, C. Rembser³⁶, A. Renardi⁴⁸, M. Renda^{27b}, M. B. Rendel¹⁰⁹, F. Renner⁴⁸, A. G. Rennie⁵⁹, S. Resconi^{70a}, M. Ressegotti^{57a,57b}, E. D. Resseguie^{17a}, S. Rettie³⁶, B. Reynolds¹¹⁸, E. Reynolds^{17a}, M. Rezaei Estabragh¹⁷⁰, O. L. Rezanova³⁷, P. Reznicek¹³², E. Ricci^{77a,77b}, R. Richter¹⁰⁹, S. Richter^{47a,47b}, E. Richter-Was^{84b}, M. Ridel¹²⁶, P. Rieck¹¹⁶, P. Riedler³⁶, M. Rijssenbeek¹⁴⁴, A. Rimoldi^{72a,72b}, M. Rimoldi⁴⁸, L. Rinaldi^{23a,23b}, T. T. Rinn²⁹, M. P. Rinnagel¹⁰⁸, G. Ripellino¹⁴³, I. Riu¹³, P. Rivadeneira⁴⁸, J. C. Rivera Vergara¹⁶⁴, F. Rizatdinova¹²⁰, E. Rizvi⁹³, C. Rizzi⁵⁶, B. A. Roberts¹⁶⁶, B. R. Roberts^{17a}, S. H. Robertson^{103,w}, M. Robin⁴⁸, D. Robinson³², C. M. Robles Gajardo^{136f}, M. Robles Manzano⁹⁹, A. Robson⁵⁹, A. Rocchi^{75a,75b}, C. Roda^{73a,73b}, S. Rodriguez Bosca^{63a}, Y. Rodriguez Garcia^{22a}, A. Rodriguez Rodriguez⁵⁴, A. M. Rodríguez Vera^{155b}, S. Roe³⁶, J. T. Roemer¹⁵⁹, A. R. Roepe-Gier¹¹⁹, J. Roggel¹⁷⁰, O. Röhne¹²⁴, R. A. Rojas¹⁶⁴, B. Roland⁵⁴, C. P. A. Roland⁶⁷, J. Roloff²⁹, A. Romaniouk³⁷, E. Romano^{72a,72b}, M. Romano^{23b}, A. C. Romero Hernandez¹⁶¹, N. Rompotis⁹¹, L. Roos¹²⁶, S. Rosati^{74a}, B. J. Rosser³⁹, E. Rossi⁴, E. Rossi^{71a,71b}, L. P. Rossi^{57b}, L. Rossini⁴⁸, R. Rosten¹¹⁸, M. Rotaru^{27b}, B. Rottler⁵⁴, D. Rousseau⁶⁶, D. Rouso³², G. Rovelli^{72a,72b}, A. Roy¹⁶¹, A. Rozanov¹⁰¹, Y. Rozen¹⁴⁹, X. Ruan^{33g}, A. Rubio Jimenez¹⁶², A. J. Ruby⁹¹, V. H. Ruelas Rivera¹⁸, T. A. Ruggeri¹, F. Rühr⁵⁴, A. Ruiz-Martinez¹⁶², A. Rummler³⁶, Z. Rurikova⁵⁴, N. A. Rusakovich³⁸, H. L. Russell¹⁶⁴, J. P. Rutherford⁷, K. Rybacki⁹⁰, M. Rybar¹³², E. B. Rye¹²⁴, A. Ryzhov³⁷, J. A. Sabater Iglesias⁵⁶, P. Sabatini¹⁶², L. Sabetta^{74a,74b}, H. F.-W. Sadrozinski¹³⁵, F. Safai Tehrani^{74a}, B. Safarzadeh Samani¹⁴⁵, M. Safdari¹⁴², S. Saha¹⁰³, M. Sahinsky¹⁰⁹, M. Saimpert¹³⁴, M. Saito¹⁵², T. Saito¹⁵², D. Salamani³⁶, G. Salamanna^{76a,76b}, A. Salnikov¹⁴², J. Salt¹⁶², A. Salvador Salas¹³, D. Salvatore^{43a,43b}, F. Salvatore¹⁴⁵, A. Salzburger³⁶, D. Sammel⁵⁴, D. Sampsonidis¹⁵¹, D. Sampsonidou^{62c,62d}, J. Sánchez¹⁶², A. Sanchez Pineda⁴, V. Sanchez Sebastian¹⁶², H. Sandaker¹²⁴, C. O. Sander⁴⁸, J. A. Sandesara¹⁰², M. Sandhoff¹⁷⁰, C. Sandoval^{22b}, D. P. C. Sankey¹³³, A. Sansoni⁵³, L. Santi^{74a,74b}, C. Santoni⁴⁰, H. Santos^{129a,129b}, S. N. Santpur^{17a}, A. Santra¹⁶⁸, K. A. Saoucha¹³⁸, J. G. Saraiva^{129a,129d}, J. Sardain⁷, O. Sasaki⁸², K. Sato¹⁵⁶, C. Sauer^{63b}, F. Sauerburger⁵⁴, E. Sauvan⁴, P. Savard^{154,ac}, R. Sawada¹⁵², C. Sawyer¹³³, L. Sawyer⁹⁶, I. Sayago Galvan¹⁶², C. Sbarra^{23b}, A. Sbrizzi^{23a,23b}, T. Scanlon⁹⁵, J. Schaarschmidt¹³⁷, P. Schacht¹⁰⁹, D. Schaefer³⁹, U. Schäfer⁹⁹, A. C. Schaffer⁶⁶, D. Schaile¹⁰⁸, R. D. Schamberger¹⁴⁴, E. Schane1¹⁰⁸, C. Scharf¹⁸, M. M. Schefer¹⁹, V. A. Schegelsky³⁷, D. Scheirich¹³², F. Schenck¹⁸, M. Schernau¹⁵⁹, C. Scheulen⁵⁵, C. Schiavi^{57a,57b}, Z. M. Schillaci²⁶, E. J. Schioppa^{69a,69b}, M. Schioppa^{43a,43b}, B. Schlag⁹⁹, K. E. Schleicher⁵⁴, S. Schlenker³⁶, M. A. Schmidt¹⁷⁰, K. Schmieden⁹⁹, C. Schmitt⁹⁹, S. Schmitt⁴⁸, L. Schoeffel¹³⁴, A. Schoening^{63b}, P. G. Scholer⁵⁴, E. Schopf¹²⁵, M. Schott⁹⁹, J. Schovancova³⁶, S. Schramm⁵⁶, F. Schroeder¹⁷⁰, H.-C. Schultz-Coulon^{63a}, M. Schumacher⁵⁴, B. A. Schumm¹³⁵, Ph. Schune¹³⁴, A. Schwartzman¹⁴², T. A. Schwarz¹⁰⁵, Ph. Schwemling¹³⁴, R. Schwienhorst¹⁰⁶, A. Sciandra¹³⁵, G. Sciolla²⁶, F. Scuri^{73a}, F. Scutti¹⁰⁴, C. D. Sebastiani⁹¹, K. Sedlaczek⁴⁹, P. Seema¹⁸, S. C. Seidel¹¹¹, A. Seiden¹³⁵, B. D. Seidlitz⁴¹, T. Seiss³⁹, C. Seitz⁴⁸, J. M. Seixas^{81b}, G. Sekhniaidze^{71a}, S. J. Sekula⁴⁴, L. Selem⁴, N. Semprini-Cesari^{23a,23b}, S. Sen⁵¹, D. Sengupta⁵⁶, V. Senthilkumar¹⁶², L. Serin⁶⁶, L. Serkin^{68a,68b}, M. Sessa^{76a,76b}, H. Severini¹¹⁹, S. Sevova¹⁴², F. Sforza^{57a,57b}, A. Sfyrlla⁵⁶, E. Shabalina⁵⁵, R. Shaheen¹⁴³, J. D. Shahinian¹²⁷, N. W. Shaikh^{47a,47b}, D. Shaked Renous¹⁶⁸, L. Y. Shan^{14a}, M. Shapiro^{17a}, A. Sharma³⁶

A. S. Sharma¹⁶³, P. Sharma⁷⁹, S. Sharma⁴⁸, P. B. Shatalov³⁷, K. Shaw¹⁴⁵, S. M. Shaw¹⁰⁰, Q. Shen^{62c,5}, P. Sherwood⁹⁵, L. Shi⁹⁵, C. O. Shimmin¹⁷¹, Y. Shimogama¹⁶⁷, J. D. Shinner⁹⁴, I. P. J. Shipsey¹²⁵, S. Shirabe⁶⁰, M. Shiyakova³⁸, J. Shlomi¹⁶⁸, M. J. Shochet³⁹, J. Shojaii¹⁰⁴, D. R. Shope¹²⁴, S. Shrestha^{118,ag}, E. M. Shrif^{33g}, M. J. Shroff¹⁶⁴, P. Sicho¹³⁰, A. M. Sickles¹⁶¹, E. Sideras Haddad^{33g}, A. Sidoti^{23b}, F. Siegert⁵⁰, Dj. Sijacki¹⁵, R. Sikora^{84a}, F. Sili⁸⁹, J. M. Silva²⁰, M. V. Silva Oliveira³⁶, S. B. Silverstein^{47a}, S. Simion⁶⁶, R. Simoniello³⁶, E. L. Simpson⁵⁹, N. D. Simpson⁹⁷, S. Simsek^{21d}, S. Sindhu⁵⁵, P. Sinervo¹⁵⁴, V. Sinetckii³⁷, S. Singh¹⁴¹, S. Singh¹⁵⁴, S. Sinha⁴⁸, S. Sinha^{33g}, M. Sioli^{23a,23b}, I. Siral³⁶, S. Yu. Sivoklov^{37,*}, J. Sjölin^{47a,47b}, A. Skaf⁵⁵, E. Skorda⁹⁷, P. Skubic¹¹⁹, M. Slawinska⁸⁵, V. Smakhtin¹⁶⁸, B. H. Smart¹³³, J. Smiesko³⁶, S. Yu. Smirnov³⁷, Y. Smirnov³⁷, L. N. Smirnova^{37,a}, O. Smirnova⁹⁷, A. C. Smith⁴¹, E. A. Smith³⁹, H. A. Smith¹²⁵, J. L. Smith⁹¹, R. Smith¹⁴², M. Smizanska⁹⁰, K. Smolek¹³¹, A. Smykiewicz⁸⁵, A. A. Snesarev³⁷, H. L. Snoek¹¹³, S. Snyder²⁹, R. Sobie^{164,w}, A. Soffer¹⁵⁰, C. A. Solans Sanchez³⁶, E. Yu. Soldatov³⁷, U. Soldevila¹⁶², A. A. Solodkov³⁷, S. Solomon⁵⁴, A. Soloshenko³⁸, K. Solovieva⁵⁴, O. V. Solovyanov³⁷, V. Solovyev³⁷, P. Sommer³⁶, A. Sonay¹³, W. Y. Song^{155b}, A. Sopczak¹³¹, A. L. Soppio⁹⁵, F. Sopkova^{28b}, V. Sothilingam^{63a}, S. Sottocornola^{72a,72b}, R. Soualah^{115b}, Z. Soumami^{35e}, D. South⁴⁸, S. Spagnolo^{69a,69b}, M. Spalla¹⁰⁹, F. Spanò⁹⁴, D. Sperlich⁵⁴, G. Spigo³⁶, M. Spina¹⁴⁵, S. Spinali⁹⁰, D. P. Spiteri⁵⁹, M. Spousta¹³², E. J. Staats³⁴, A. Stabile^{70a,70b}, R. Stamen^{63a}, M. Stamenkovic¹¹³, A. Stampeki²⁰, M. Standke²⁴, E. Stanecka⁸⁵, M. V. Stange⁵⁰, B. Stanislaus^{17a}, M. M. Stanitzki⁴⁸, M. Stankaityte¹²⁵, B. Stapf⁴⁸, E. A. Starchenko³⁷, G. H. Stark¹³⁵, J. Stark¹⁰¹, D. M. Starke^{155b}, P. Staroba¹³⁰, P. Starovoitov^{63a}, S. Stärz¹⁰³, R. Staszewski⁸⁵, G. Stavropoulos⁴⁶, J. Steentoft¹⁶⁰, P. Steinberg²⁹, A. L. Steinhebel¹²², B. Stelzer^{141,155a}, H. J. Stelzer¹²⁸, O. Stelzer-Chilton^{155a}, H. Stenzel⁵⁸, T. J. Stevenson¹⁴⁵, G. A. Stewart³⁶, M. C. Stockton³⁶, G. Stoica^{27b}, M. Stolarski^{129a}, S. Stonjek¹⁰⁹, A. Straessner⁵⁰, J. Strandberg¹⁴³, S. Strandberg^{47a,47b}, M. Strauss¹¹⁹, T. Strebler¹⁰¹, P. Strizenc^{28b}, R. Ströhmer¹⁶⁵, D. M. Strom¹²², L. R. Strom⁴⁸, R. Stroynowski⁴⁴, A. Strubig^{47a,47b}, S. A. Stucci²⁹, B. Stugu¹⁶, J. Stupak¹¹⁹, N. A. Styles⁴⁸, D. Su¹⁴², S. Su^{62a}, W. Su^{62c,62d,137}, X. Su^{62a,66}, K. Sugizaki¹⁵², V. V. Sulim³⁷, M. J. Sullivan⁹¹, D. M. S. Sultan^{77a,77b}, L. Sultanaliyeva³⁷, S. Sultansoy^{3b}, T. Sumida⁸⁶, S. Sun¹⁰⁵, S. Sun¹⁶⁹, O. Sunneborn Gudnadottir¹⁶⁰, M. R. Sutton¹⁴⁵, M. Svatos¹³⁰, M. Swiatkowski^{155a}, T. Swirski¹⁶⁵, I. Sykora^{28a}, M. Sykora¹³², T. Sykora¹³², D. Ta⁹⁹, K. Tackmann^{48,v}, A. Taffard¹⁵⁹, R. Tafirout^{155a}, J. S. Tafoya Vargas⁶⁶, R. H. M. Taibah¹²⁶, R. Takashima⁸⁷, K. Takeda⁸³, E. P. Takeva⁵², Y. Takubo⁸², M. Talby¹⁰¹, A. A. Talyshv³⁷, K. C. Tam^{64b}, N. M. Tamir¹⁵⁰, A. Tanaka¹⁵², J. Tanaka¹⁵², R. Tanaka⁶⁶, M. Tanasini^{57a,57b}, J. Tang^{62c}, Z. Tao¹⁶³, S. Tapia Araya⁸⁰, S. Tapprogge⁹⁹, A. Tarek Abouelfadl Mohamed¹⁰⁶, S. Tarem¹⁴⁹, K. Tariq^{62b}, G. Tarna^{27b,101}, G. F. Tartarelli^{70a}, P. Tas¹³², M. Tasevsky¹³⁰, E. Tassi^{43a,43b}, A. C. Tate¹⁶¹, G. Tateno¹⁵², Y. Tayalati^{35e}, G. N. Taylor¹⁰⁴, W. Taylor^{155b}, H. Teagle⁹¹, A. S. Tee¹⁶⁹, R. Teixeira De Lima¹⁴², P. Teixeira-Dias⁹⁴, J. J. Teoh¹⁵⁴, K. Terashi¹⁵², J. Terron⁹⁸, S. Terzo¹³, M. Testa⁵³, R. J. Teuscher^{154,w}, A. Thaler⁷⁸, O. Theiner⁵⁶, N. Themistokleous⁵², T. Thevenaux-Pelzer¹⁸, O. Thielmann¹⁷⁰, D. W. Thomas⁹⁴, J. P. Thomas²⁰, E. A. Thompson⁴⁸, P. D. Thompson²⁰, E. Thomson¹²⁷, E. J. Thorpe⁹³, Y. Tian⁵⁵, V. Tikhomirov^{37,a}, Yu. A. Tikhonov³⁷, S. Timoshenko³⁷, E. X. L. Ting¹, P. Tipton¹⁷¹, S. Tisserant¹⁰¹, S. H. Tlou^{33g}, A. Tmourji⁴⁰, K. Todome^{23a,23b}, S. Todorova-Nova¹³², S. Todt⁵⁰, M. Togawa⁸², J. Tojo⁸⁸, S. Tokár^{28a}, K. Tokushuku⁸², R. Tombs³², M. Tomoto^{82,110}, L. Tompkins¹⁴², K. W. Topolnicki^{84b}, P. Tornambe¹⁰², E. Torrence¹²², H. Torres⁵⁰, E. Torrón Pastor¹⁶², M. Toscani³⁰, C. Tosciri³⁹, D. R. Tovey¹³⁸, A. Traeet¹⁶, I. S. Trandafir^{27b}, T. Trefzger¹⁶⁵, A. Tricoli²⁹, I. M. Trigger^{155a}, S. Trincz-Duvold¹²⁶, D. A. Trischuk²⁶, B. Trocmé⁶⁰, A. Trofymov⁶⁶, C. Troncon^{70a}, L. Truong^{33c}, M. Trzebinski⁸⁵, A. Trzupek⁸⁵, F. Tsai¹⁴⁴, M. Tsai¹⁰⁵, A. Tsiamis¹⁵¹, P. V. Tsiareshka³⁷, S. Tsigaridas^{155a}, A. Tsirigotis^{151,t}, V. Tsiskaridze¹⁴⁴, E. G. Tskhadadze^{148a}, M. Tsopoulou¹⁵¹, Y. Tsujikawa⁸⁶, I. I. Tsukerman³⁷, V. Tsulaia^{17a}, S. Tsuno⁸², O. Tsur¹⁴⁹, D. Tsybychev¹⁴⁴, Y. Tu^{64b}, A. Tudorache^{27b}, V. Tudorache^{27b}, A. N. Tuna³⁶, S. Turchikhin³⁸, I. Turk Cakir^{3a}, R. Turra^{70a}, T. Turtuvshin³⁸, P. M. Tuts⁴¹, S. Tzamarias¹⁵¹, P. Tzani¹⁰, E. Tzovara⁹⁹, K. Uchida¹⁵², F. Ukegawa¹⁵⁶, P. A. Ulloa Poblete^{136c}, G. Unal³⁶, M. Unal¹¹, A. Undrus²⁹, G. Unel¹⁵⁹, J. Urban^{28b}, P. Urquijo¹⁰⁴, G. Usai⁸, R. Ushioda¹⁵³, M. Usman¹⁰⁷, Z. Uysal^{21b}, V. Vacek¹³¹, B. Vachon¹⁰³, K. O. H. Vadla¹²⁴, T. Vafeiadis³⁶, C. Valderanis¹⁰⁸, E. Valdes Santurio^{47a,47b}, M. Valente^{155a}, S. Valentini^{23a,23b}, A. Valero¹⁶², A. Vallier¹⁰¹, J. A. Valls Ferrer¹⁶², T. R. Van Daalen¹³⁷, P. Van Gemmeren⁶, M. Van Rijnbach^{124,36}, S. Van Stroud⁹⁵, I. Van Vulpen¹¹³, M. Vanadia^{75a,75b}, W. Vandelli³⁶, M. Vandenbroucke¹³⁴, E. R. Vandewall¹²⁰, D. Vannicola¹⁵⁰, L. Vannoli^{57a,57b}, R. Vari^{74a}, E. W. Varnes⁷, C. Varni^{17a}, T. Varol¹⁴⁷, D. Varouchas⁶⁶, L. Varriale¹⁶², K. E. Varvell¹⁴⁶

M. E. Vasile^{27b}, L. Vaslin⁴⁰, G. A. Vasquez¹⁶⁴, F. Vazeille⁴⁰, T. Vazquez Schroeder³⁶, J. Veatch³¹, V. Vecchio¹⁰⁰, M. J. Veen¹⁰², I. Veliscek¹²⁵, L. M. Veloce¹⁵⁴, F. Veloso^{129a,129c}, S. Veneziano^{74a}, A. Ventura^{69a,69b}, A. Verbytskyi¹⁰⁹, M. Verducci^{73a,73b}, C. Vergis²⁴, M. Verissimo De Araujo^{81b}, W. Verkerke¹¹³, J. C. Vermeulen¹¹³, C. Vernieri¹⁴², P. J. Verschuuren⁹⁴, M. Vessella¹⁰², M. C. Vetterli^{141,ac}, A. Vgenopoulos¹⁵¹, N. Viaux Maira^{136f}, T. Vickey¹³⁸, O. E. Vickey Boeriu¹³⁸, G. H. A. Viehhauser¹²⁵, L. Vigani^{63b}, M. Villa^{23a,23b}, M. Villaplana Perez¹⁶², E. M. Villhauer⁵², E. Vilucchi⁵³, M. G. Vinciter³⁴, G. S. Virdee²⁰, A. Vishwakarma⁵², C. Vittori^{23a,23b}, I. Vivarelli¹⁴⁵, V. Vladimirov¹⁶⁶, E. Voevodina¹⁰⁹, F. Vogel¹⁰⁸, P. Vokac¹³¹, J. Von Ahnen⁴⁸, E. Von Toerne²⁴, B. Vormwald³⁶, V. Vorobel¹³², K. Vorobev³⁷, M. Vos¹⁶², J. H. Vosseveld⁹¹, M. Vozak¹¹³, L. Vozdecky⁹³, N. Vranjes¹⁵, M. Vranjes Milosavljevic¹⁵, M. Vreeswijk¹¹³, R. Vuillermet³⁶, O. Vujinovic⁹⁹, I. Vukotic³⁹, S. Wada¹⁵⁶, C. Wagner¹⁰², W. Wagner¹⁷⁰, S. Wahdan¹⁷⁰, H. Wahlberg⁸⁹, R. Wakasa¹⁵⁶, M. Wakida¹¹⁰, V. M. Walbrecht¹⁰⁹, J. Walder¹³³, R. Walker¹⁰⁸, W. Walkowiak¹⁴⁰, A. M. Wang⁶¹, A. Z. Wang¹⁶⁹, C. Wang^{62a}, C. Wang^{62c}, H. Wang^{17a}, J. Wang^{64a}, P. Wang⁴⁴, R. -J. Wang⁹⁹, R. Wang⁶¹, R. Wang⁶, S. M. Wang¹⁴⁷, S. Wang^{62b}, T. Wang^{62a}, W. T. Wang⁷⁹, W. X. Wang^{62a}, X. Wang^{14c}, X. Wang¹⁶¹, X. Wang^{62c}, Y. Wang^{62d}, Y. Wang^{14c}, Z. Wang¹⁰⁵, Z. Wang^{51,62c,62d}, Z. Wang¹⁰⁵, A. Warburton¹⁰³, R. J. Ward²⁰, N. Warrack⁵⁹, A. T. Watson²⁰, M. F. Watson²⁰, G. Watts¹³⁷, B. M. Waugh⁹⁵, A. F. Webb¹¹, C. Weber²⁹, M. S. Weber¹⁹, S. M. Weber^{63a}, C. Wei^{62a}, Y. Wei¹²⁵, A. R. Weidberg¹²⁵, J. Weingarten⁴⁹, M. Weirich⁹⁹, C. Weiser⁵⁴, C. J. Wells⁴⁸, T. Wenaus²⁹, B. Wendland⁴⁹, T. Wengler³⁶, N. S. Wenke¹⁰⁹, N. Wermes²⁴, M. Wessels^{63a}, K. Whalen¹²², A. M. Wharton⁹⁰, A. S. White⁶¹, A. White⁸, M. J. White¹, D. Whiteson¹⁵⁹, L. Wickremasinghe¹²³, W. Wiedenmann¹⁶⁹, C. Wiel⁵⁰, M. Wielers¹³³, N. Wieseotte⁹⁹, C. Wiglesworth⁴², L. A. M. Wiik-Fuchs⁵⁴, D. J. Wilbern¹¹⁹, H. G. Wilkens³⁶, D. M. Williams⁴¹, H. H. Williams¹²⁷, S. Williams³², S. Willocq¹⁰², P. J. Windischhofer¹²⁵, F. Winklmeier¹²², B. T. Winter⁵⁴, J. K. Winter¹⁰⁰, M. Wittgen¹⁴², M. Wobisch⁹⁶, R. Wölker¹²⁵, J. Wollrath¹⁵⁹, M. W. Wolter⁸⁵, H. Wolters^{129a,129c}, V. W. S. Wong¹⁶³, A. F. Wongel⁴⁸, S. D. Worm⁴⁸, B. K. Wosiek⁸⁵, K. W. Woźniak⁸⁵, K. Wraight⁵⁹, J. Wu^{14a,14d}, M. Wu^{64a}, M. Wu¹¹², S. L. Wu¹⁶⁹, X. Wu⁵⁶, Y. Wu^{62a}, Z. Wu^{62a,134}, J. Wuerzinger¹²⁵, T. R. Wyatt¹⁰⁰, B. M. Wynne⁵², S. Xella⁴², L. Xia^{14c}, M. Xia^{14b}, J. Xiang^{64c}, X. Xiao¹⁰⁵, M. Xie^{62a}, X. Xie^{62a}, S. Xin^{14a,14d}, J. Xiong^{17a}, I. Xiotidis¹⁴⁵, D. Xu^{14a}, H. Xu^{62a}, H. Xu^{62a}, L. Xu^{62a}, R. Xu¹²⁷, T. Xu¹⁰⁵, W. Xu¹⁰⁵, Y. Xu^{14b}, Z. Xu^{62b}, Z. Xu^{14a}, B. Yabsley¹⁴⁶, S. Yacoub^{33a}, N. Yamaguchi⁸⁸, Y. Yamaguchi¹⁵³, H. Yamauchi¹⁵⁶, T. Yamazaki^{17a}, Y. Yamazaki⁸³, J. Yan^{62c}, S. Yan¹²⁵, Z. Yan²⁵, H. J. Yang^{62c,62d}, H. T. Yang^{17a}, S. Yang^{62a}, T. Yang^{64c}, X. Yang^{62a}, X. Yang^{14a}, Y. Yang⁴⁴, Z. Yang^{62a,105}, W.-M. Yao^{17a}, Y. C. Yap⁴⁸, H. Ye^{14c}, H. Ye⁵⁵, J. Ye⁴⁴, S. Ye²⁹, X. Ye^{62a}, Y. Yeh⁹⁵, I. Yeletsikh³⁸, B. K. Yeo^{17a}, M. R. Yexley⁹⁰, P. Yin⁴¹, K. Yorita¹⁶⁷, C. J. S. Young⁵⁴, C. Young¹⁴², M. Yuan¹⁰⁵, R. Yuan^{62b,k}, L. Yue⁹⁵, X. Yue^{63a}, M. Zaazoua^{35e}, B. Zabinski⁸⁵, E. Zaid⁵², T. Zakareishvili^{148b}, N. Zakharchuk³⁴, S. Zambito⁵⁶, J. A. Zamora Saa^{136d}, J. Zang¹⁵², D. Zanzi⁵⁴, O. Zaplatilek¹³¹, S. V. Zeiβner⁴⁹, C. Zeitnitz¹⁷⁰, J. C. Zeng¹⁶¹, D. T. Zenger Jr²⁶, O. Zenin³⁷, T. Ženiš^{28a}, S. Zenz⁹³, S. Zerradi^{35a}, D. Zerwas⁶⁶, B. Zhang^{14c}, D. F. Zhang¹³⁸, G. Zhang^{14b}, J. Zhang^{62b}, J. Zhang⁶, K. Zhang^{14a,14d}, L. Zhang^{14c}, P. Zhang^{14a,14d}, R. Zhang¹⁶⁹, S. Zhang¹⁰⁵, T. Zhang¹⁵², X. Zhang^{62c}, X. Zhang^{62b}, Y. Zhang^{5,62c}, Z. Zhang^{17a}, Z. Zhang⁶⁶, H. Zhao¹³⁷, P. Zhao⁵¹, T. Zhao^{62b}, Y. Zhao¹³⁵, Z. Zhao^{62a}, A. Zhemchugov³⁸, X. Zheng^{62a}, Z. Zheng¹⁴², D. Zhong¹⁶¹, B. Zhou¹⁰⁵, C. Zhou¹⁶⁹, H. Zhou⁷, N. Zhou^{62c}, Y. Zhou⁷, C. G. Zhu^{62b}, C. Zhu^{14a,14d}, H. L. Zhu^{62a}, H. Zhu^{14a}, J. Zhu¹⁰⁵, Y. Zhu^{62c}, Y. Zhu^{62a}, X. Zhuang^{14a}, K. Zhukov³⁷, V. Zhulanov³⁷, N. I. Zimine³⁸, J. Zinsler^{63b}, M. Ziolkowski¹⁴⁰, L. Živković¹⁵, A. Zoccoli^{23a,23b}, K. Zoch⁵⁶, T. G. Zorbas¹³⁸, O. Zormpa⁴⁶, W. Zou⁴¹, L. Zwalinski³⁶

¹ Department of Physics, University of Adelaide, Adelaide, Australia

² Department of Physics, University of Alberta, Edmonton, AB, Canada

³ (a)Department of Physics, Ankara University, Ankara, Türkiye; (b)Division of Physics, TOBB University of Economics and Technology, Ankara, Türkiye

⁴ LAPP, Univ. Savoie Mont Blanc, CNRS/IN2P3, Annecy, France

⁵ APC, Université Paris Cité, CNRS/IN2P3, Paris, France

⁶ High Energy Physics Division, Argonne National Laboratory, Argonne, IL, USA

⁷ Department of Physics, University of Arizona, Tucson, AZ, USA

⁸ Department of Physics, University of Texas at Arlington, Arlington, TX, USA

⁹ Physics Department, National and Kapodistrian University of Athens, Athens, Greece

- 10 Physics Department, National Technical University of Athens, Zografou, Greece
- 11 Department of Physics, University of Texas at Austin, Austin, TX, USA
- 12 Institute of Physics, Azerbaijan Academy of Sciences, Baku, Azerbaijan
- 13 Institut de Física d'Altes Energies (IFAE), Barcelona Institute of Science and Technology, Barcelona, Spain
- 14 (a)Institute of High Energy Physics, Chinese Academy of Sciences, Beijing, China; (b)Physics Department, Tsinghua University, Beijing, China; (c)Department of Physics, Nanjing University, Nanjing, China; (d)University of Chinese Academy of Science (UCAS), Beijing, China
- 15 Institute of Physics, University of Belgrade, Belgrade, Serbia
- 16 Department for Physics and Technology, University of Bergen, Bergen, Norway
- 17 (a)Physics Division, Lawrence Berkeley National Laboratory, Berkeley, CA, USA; (b)University of California, Berkeley, CA, USA
- 18 Institut für Physik, Humboldt Universität zu Berlin, Berlin, Germany
- 19 Albert Einstein Center for Fundamental Physics and Laboratory for High Energy Physics, University of Bern, Bern, Switzerland
- 20 School of Physics and Astronomy, University of Birmingham, Birmingham, UK
- 21 (a)Department of Physics, Bogazici University, Istanbul, Türkiye; (b)Department of Physics Engineering, Gaziantep University, Gaziantep, Türkiye; (c)Department of Physics, Istanbul University, Istanbul, Türkiye; (d)Istinye University, Sariyer, Istanbul, Türkiye
- 22 (a)Facultad de Ciencias y Centro de Investigaciones, Universidad Antonio Nariño, Bogotá, Colombia; (b)Departamento de Física, Universidad Nacional de Colombia, Bogotá, Colombia
- 23 (a)Dipartimento di Fisica e Astronomia A. Righi, Università di Bologna, Bologna, Italy; (b)INFN Sezione di Bologna, Bologna, Italy
- 24 Physikalisches Institut, Universität Bonn, Bonn, Germany
- 25 Department of Physics, Boston University, Boston, MA, USA
- 26 Department of Physics, Brandeis University, Waltham, MA, USA
- 27 (a)Transilvania University of Brasov, Brasov, Romania; (b)Horia Hulubei National Institute of Physics and Nuclear Engineering, Bucharest, Romania; (c)Department of Physics, Alexandru Ioan Cuza University of Iasi, Iasi, Romania; (d)Physics Department, National Institute for Research and Development of Isotopic and Molecular Technologies, Cluj-Napoca, Romania; (e)University Politehnica Bucharest, Bucharest, Romania; (f)West University in Timisoara, Timisoara, Romania; (g)Faculty of Physics, University of Bucharest, Bucharest, Romania
- 28 (a)Faculty of Mathematics, Physics and Informatics, Comenius University, Bratislava, Slovak Republic; (b)Department of Subnuclear Physics, Institute of Experimental Physics of the Slovak Academy of Sciences, Kosice, Slovak Republic
- 29 Physics Department, Brookhaven National Laboratory, Upton, NY, USA
- 30 Departamento de Física, y CONICET, Facultad de Ciencias Exactas y Naturales, Instituto de Física de Buenos Aires (IFIBA), Universidad de Buenos Aires, Buenos Aires, Argentina
- 31 California State University, Long Beach, CA, USA
- 32 Cavendish Laboratory, University of Cambridge, Cambridge, UK
- 33 (a)Department of Physics, University of Cape Town, Cape Town, South Africa; (b)iThemba Labs, Western Cape, South Africa; (c)Department of Mechanical Engineering Science, University of Johannesburg, Johannesburg, South Africa; (d)National Institute of Physics, University of the Philippines Diliman (Philippines), Quezon City, South Africa; (e)Department of Physics, University of South Africa, Pretoria, South Africa; (f)University of Zululand, KwaDlangezwa, South Africa; (g)School of Physics, University of the Witwatersrand, Johannesburg, South Africa
- 34 Department of Physics, Carleton University, Ottawa, ON, Canada
- 35 (a)Faculté des Sciences Ain Chock, Réseau Universitaire de Physique des Hautes Energies-Université Hassan II, Casablanca, Morocco; (b)Faculté des Sciences, Université Ibn-Tofail, Kenitra, Morocco; (c)Faculté des Sciences Semlalia, Université Cadi Ayyad, LPHEA-Marrakech, Marrakesh, Morocco; (d)LPMR, Faculté des Sciences, Université Mohamed Premier, Oujda, Morocco; (e)Faculté des sciences, Université Mohammed V, Rabat, Morocco; (f)Institute of Applied Physics, Mohammed VI Polytechnic University, Ben Guerir, Morocco
- 36 CERN, Geneva, Switzerland
- 37 Affiliated with an institute covered by a cooperation agreement with CERN, Geneva, Switzerland
- 38 Affiliated with an international laboratory covered by a cooperation agreement with CERN, Geneva, Switzerland
- 39 Enrico Fermi Institute, University of Chicago, Chicago, IL, USA
- 40 LPC, Université Clermont Auvergne, CNRS/IN2P3, Clermont-Ferrand, France

- 41 Nevis Laboratory, Columbia University, Irvington, NY, USA
- 42 Niels Bohr Institute, University of Copenhagen, Copenhagen, Denmark
- 43 (a)Dipartimento di Fisica, Università della Calabria, Rende, Italy; (b)INFN Gruppo Collegato di Cosenza, Laboratori Nazionali di Frascati, Frascati, Italy
- 44 Physics Department, Southern Methodist University, Dallas, TX, USA
- 45 Physics Department, University of Texas at Dallas, Richardson, TX, USA
- 46 National Centre for Scientific Research “Demokritos”, Agia Paraskevi, Greece
- 47 (a)Department of Physics, Stockholm University, Stockholm, Sweden; (b)Oskar Klein Centre, Stockholm, Sweden
- 48 Deutsches Elektronen-Synchrotron DESY, Hamburg and Zeuthen, Germany
- 49 Fakultät Physik , Technische Universität Dortmund, Dortmund, Germany
- 50 Institut für Kern- und Teilchenphysik, Technische Universität Dresden, Dresden, Germany
- 51 Department of Physics, Duke University, Durham, NC, USA
- 52 SUPA-School of Physics and Astronomy, University of Edinburgh, Edinburgh, UK
- 53 INFN e Laboratori Nazionali di Frascati, Frascati, Italy
- 54 Physikalisches Institut, Albert-Ludwigs-Universität Freiburg, Freiburg, Germany
- 55 II. Physikalisches Institut, Georg-August-Universität Göttingen, Göttingen, Germany
- 56 Département de Physique Nucléaire et Corpusculaire, Université de Genève, Genève, Switzerland
- 57 (a)Dipartimento di Fisica, Università di Genova, Genoa, Italy; (b)INFN Sezione di Genova, Genoa, Italy
- 58 II. Physikalisches Institut, Justus-Liebig-Universität Giessen, Giessen, Germany
- 59 SUPA-School of Physics and Astronomy, University of Glasgow, Glasgow, UK
- 60 LPSC, Université Grenoble Alpes, CNRS/IN2P3, Grenoble INP, Grenoble, France
- 61 Laboratory for Particle Physics and Cosmology, Harvard University, Cambridge, MA, USA
- 62 (a)Department of Modern Physics and State Key Laboratory of Particle Detection and Electronics, University of Science and Technology of China, Hefei, China; (b)Institute of Frontier and Interdisciplinary Science and Key Laboratory of Particle Physics and Particle Irradiation (MOE), Shandong University, Qingdao, China; (c)School of Physics and Astronomy, Shanghai Jiao Tong University, Key Laboratory for Particle Astrophysics and Cosmology (MOE), SKLPPC, Shanghai, China; (d)Tsung-Dao Lee Institute, Shanghai, China
- 63 (a)Kirchhoff-Institut für Physik, Ruprecht-Karls-Universität Heidelberg, Heidelberg, Germany; (b)Physikalisches Institut, Ruprecht-Karls-Universität Heidelberg, Heidelberg, Germany
- 64 (a)Department of Physics, Chinese University of Hong Kong, Shatin N.T., Hong Kong, China; (b)Department of Physics, University of Hong Kong, Hong Kong, China; (c)Department of Physics and Institute for Advanced Study, Hong Kong University of Science and Technology, Clear Water Bay, Kowloon, Hong Kong, China
- 65 Department of Physics, National Tsing Hua University, Hsinchu, Taiwan
- 66 IJCLab, Université Paris-Saclay, CNRS/IN2P3, 91405 Orsay, France
- 67 Department of Physics, Indiana University, Bloomington, IN, USA
- 68 (a)INFN Gruppo Collegato di Udine, Sezione di Trieste, Udine, Italy; (b)ICTP, Trieste, Italy; (c)Dipartimento Politecnico di Ingegneria e Architettura, Università di Udine, Udine, Italy
- 69 (a)INFN Sezione di Lecce, Lecce, Italy; (b)Dipartimento di Matematica e Fisica, Università del Salento, Lecce, Italy
- 70 (a)INFN Sezione di Milano, Milan, Italy; (b)Dipartimento di Fisica, Università di Milano, Milan, Italy
- 71 (a)INFN Sezione di Napoli, Naples, Italy; (b)Dipartimento di Fisica, Università di Napoli, Naples, Italy
- 72 (a)INFN Sezione di Pavia, Pavia, Italy; (b)Dipartimento di Fisica, Università di Pavia, Pavia, Italy
- 73 (a)INFN Sezione di Pisa, Pisa, Italy; (b)Dipartimento di Fisica E. Fermi, Università di Pisa, Pisa, Italy
- 74 (a)INFN Sezione di Roma, Rome, Italy; (b)Dipartimento di Fisica, Sapienza Università di Roma, Rome, Italy
- 75 (a)INFN Sezione di Roma Tor Vergata, Rome, Italy; (b)Dipartimento di Fisica, Università di Roma Tor Vergata, Rome, Italy
- 76 (a)INFN Sezione di Roma Tre, Rome, Italy; (b)Dipartimento di Matematica e Fisica, Università Roma Tre, Rome, Italy
- 77 (a)INFN-TIFPA, Trento, Italy; (b)Università degli Studi di Trento, Trento, Italy
- 78 Department of Astro and Particle Physics, Universität Innsbruck, Innsbruck, Austria
- 79 University of Iowa, Iowa City, IA, USA
- 80 Department of Physics and Astronomy, Iowa State University, Ames, IA, USA
- 81 (a)Departamento de Engenharia Elétrica, Universidade Federal de Juiz de Fora (UFJF), Juiz de Fora, Brazil; (b)Universidade Federal do Rio De Janeiro COPPE/EE/IF, Rio de Janeiro, Brazil; (c)Instituto de Física, Universidade de São Paulo, São Paulo, Brazil; (d)Rio de Janeiro State University, Rio de Janeiro, Brazil

- 82 KEK, High Energy Accelerator Research Organization, Tsukuba, Japan
- 83 Graduate School of Science, Kobe University, Kobe, Japan
- 84 (a) AGH University of Science and Technology, Faculty of Physics and Applied Computer Science, Kraków, Poland; (b) Marian Smoluchowski Institute of Physics, Jagiellonian University, Kraków, Poland
- 85 Institute of Nuclear Physics Polish Academy of Sciences, Kraków, Poland
- 86 Faculty of Science, Kyoto University, Kyoto, Japan
- 87 Kyoto University of Education, Kyoto, Japan
- 88 Research Center for Advanced Particle Physics and Department of Physics, Kyushu University, Fukuoka, Japan
- 89 Instituto de Física La Plata, Universidad Nacional de La Plata and CONICET, La Plata, Argentina
- 90 Physics Department, Lancaster University, Lancaster, UK
- 91 Oliver Lodge Laboratory, University of Liverpool, Liverpool, UK
- 92 Department of Experimental Particle Physics, Jožef Stefan Institute and Department of Physics, University of Ljubljana, Ljubljana, Slovenia
- 93 School of Physics and Astronomy, Queen Mary University of London, London, UK
- 94 Department of Physics, Royal Holloway University of London, Egham, UK
- 95 Department of Physics and Astronomy, University College London, London, UK
- 96 Louisiana Tech University, Ruston, LA, USA
- 97 Fysiska Institutionen, Lunds Universitet, Lund, Sweden
- 98 Departamento de Física Teórica C-15 and CIAFF, Universidad Autónoma de Madrid, Madrid, Spain
- 99 Institut für Physik, Universität Mainz, Mainz, Germany
- 100 School of Physics and Astronomy, University of Manchester, Manchester, UK
- 101 CPPM, Aix-Marseille Université, CNRS/IN2P3, Marseille, France
- 102 Department of Physics, University of Massachusetts, Amherst, MA, USA
- 103 Department of Physics, McGill University, Montreal, QC, Canada
- 104 School of Physics, University of Melbourne, Melbourne, VIC, Australia
- 105 Department of Physics, University of Michigan, Ann Arbor, MI, USA
- 106 Department of Physics and Astronomy, Michigan State University, East Lansing, MI, USA
- 107 Group of Particle Physics, University of Montreal, Montreal, QC, Canada
- 108 Fakultät für Physik, Ludwig-Maximilians-Universität München, Munich, Germany
- 109 Max-Planck-Institut für Physik (Werner-Heisenberg-Institut), Munich, Germany
- 110 Graduate School of Science and Kobayashi-Maskawa Institute, Nagoya University, Nagoya, Japan
- 111 Department of Physics and Astronomy, University of New Mexico, Albuquerque, NM, USA
- 112 Institute for Mathematics, Astrophysics and Particle Physics, Radboud University/Nikhef, Nijmegen, The Netherlands
- 113 Nikhef National Institute for Subatomic Physics and University of Amsterdam, Amsterdam, The Netherlands
- 114 Department of Physics, Northern Illinois University, DeKalb, IL, USA
- 115 (a) New York University Abu Dhabi, Abu Dhabi, United Arab Emirates; (b) University of Sharjah, Sharjah, United Arab Emirates
- 116 Department of Physics, New York University, New York, NY, USA
- 117 Ochanomizu University, Otsuka, Bunkyo-ku, Tokyo, Japan
- 118 Ohio State University, Columbus, OH, USA
- 119 Homer L. Dodge Department of Physics and Astronomy, University of Oklahoma, Norman, OK, USA
- 120 Department of Physics, Oklahoma State University, Stillwater, OK, USA
- 121 Palacký University, Joint Laboratory of Optics, Olomouc, Czech Republic
- 122 Institute for Fundamental Science, University of Oregon, Eugene, OR, USA
- 123 Graduate School of Science, Osaka University, Osaka, Japan
- 124 Department of Physics, University of Oslo, Oslo, Norway
- 125 Department of Physics, Oxford University, Oxford, UK
- 126 LPNHE, Sorbonne Université, Université Paris Cité, CNRS/IN2P3, Paris, France
- 127 Department of Physics, University of Pennsylvania, Philadelphia, PA, USA
- 128 Department of Physics and Astronomy, University of Pittsburgh, Pittsburgh, PA, USA
- 129 (a) Laboratório de Instrumentação e Física Experimental de Partículas-LIP, Lisbon, Portugal; (b) Departamento de Física, Faculdade de Ciências, Universidade de Lisboa, Lisbon, Portugal; (c) Departamento de Física, Universidade de Coimbra, Coimbra, Portugal; (d) Centro de Física Nuclear da Universidade de Lisboa, Lisbon, Portugal; (e) Departamento de Física,

- Universidade do Minho, Braga, Portugal; ^(f)Departamento de Física Teórica y del Cosmos, Universidad de Granada, Granada, Spain; ^(g)Departamento de Física, Instituto Superior Técnico, Universidade de Lisboa, Lisbon, Portugal
- 130 Institute of Physics of the Czech Academy of Sciences, Prague, Czech Republic
- 131 Czech Technical University in Prague, Prague, Czech Republic
- 132 Faculty of Mathematics and Physics, Charles University, Prague, Czech Republic
- 133 Particle Physics Department, Rutherford Appleton Laboratory, Didcot, UK
- 134 IRFU, CEA, Université Paris-Saclay, Gif-sur-Yvette, France
- 135 Santa Cruz Institute for Particle Physics, University of California Santa Cruz, Santa Cruz, CA, USA
- 136 ^(a)Departamento de Física, Pontificia Universidad Católica de Chile, Santiago, Chile; ^(b)Millennium Institute for Subatomic physics at high energy frontier (SAPHIR), Santiago, Chile; ^(c)Instituto de Investigación Multidisciplinario en Ciencia y Tecnología, y Departamento de Física, Universidad de La Serena, Chile; ^(d)Universidad Andres Bello, Department of Physics, Santiago, Chile; ^(e)Instituto de Alta Investigación, Universidad de Tarapacá, Arica, Chile; ^(f)Departamento de Física, Universidad Técnica Federico Santa María, Valparaíso, Chile
- 137 Department of Physics, University of Washington, Seattle, WA, USA
- 138 Department of Physics and Astronomy, University of Sheffield, Sheffield, UK
- 139 Department of Physics, Shinshu University, Nagano, Japan
- 140 Department Physik, Universität Siegen, Siegen, Germany
- 141 Department of Physics, Simon Fraser University, Burnaby, BC, Canada
- 142 SLAC National Accelerator Laboratory, Stanford, CA, USA
- 143 Department of Physics, Royal Institute of Technology, Stockholm, Sweden
- 144 Departments of Physics and Astronomy, Stony Brook University, Stony Brook, NY, USA
- 145 Department of Physics and Astronomy, University of Sussex, Brighton, UK
- 146 School of Physics, University of Sydney, Sydney, Australia
- 147 Institute of Physics, Academia Sinica, Taipei, Taiwan
- 148 ^(a)E. Andronikashvili Institute of Physics, Iv. Javakhishvili Tbilisi State University, Tbilisi, Georgia; ^(b)High Energy Physics Institute, Tbilisi State University, Tbilisi, Georgia; ^(c)University of Georgia, Tbilisi, Georgia
- 149 Department of Physics, Technion, Israel Institute of Technology, Haifa, Israel
- 150 Raymond and Beverly Sackler School of Physics and Astronomy, Tel Aviv University, Tel Aviv, Israel
- 151 Department of Physics, Aristotle University of Thessaloniki, Thessaloniki, Greece
- 152 International Center for Elementary Particle Physics and Department of Physics, University of Tokyo, Tokyo, Japan
- 153 Department of Physics, Tokyo Institute of Technology, Tokyo, Japan
- 154 Department of Physics, University of Toronto, Toronto, ON, Canada
- 155 ^(a)TRIUMF, Vancouver, BC, Canada; ^(b)Department of Physics and Astronomy, York University, Toronto, ON, Canada
- 156 Division of Physics and Tomonaga Center for the History of the Universe, Faculty of Pure and Applied Sciences, University of Tsukuba, Tsukuba, Japan
- 157 Department of Physics and Astronomy, Tufts University, Medford, MA, USA
- 158 United Arab Emirates University, Al Ain, United Arab Emirates
- 159 Department of Physics and Astronomy, University of California Irvine, Irvine, CA, USA
- 160 Department of Physics and Astronomy, University of Uppsala, Uppsala, Sweden
- 161 Department of Physics, University of Illinois, Urbana, IL, USA
- 162 Instituto de Física Corpuscular (IFIC), Centro Mixto Universidad de Valencia-CSIC, Valencia, Spain
- 163 Department of Physics, University of British Columbia, Vancouver, BC, Canada
- 164 Department of Physics and Astronomy, University of Victoria, Victoria, BC, Canada
- 165 Fakultät für Physik und Astronomie, Julius-Maximilians-Universität Würzburg, Würzburg, Germany
- 166 Department of Physics, University of Warwick, Coventry, UK
- 167 Waseda University, Tokyo, Japan
- 168 Department of Particle Physics and Astrophysics, Weizmann Institute of Science, Rehovot, Israel
- 169 Department of Physics, University of Wisconsin, Madison, WI, USA
- 170 Fakultät für Mathematik und Naturwissenschaften, Fachgruppe Physik, Bergische Universität Wuppertal, Wuppertal, Germany
- 171 Department of Physics, Yale University, New Haven, CT, USA

^a Also Affiliated with an institute covered by a cooperation agreement with CERN, Geneva, Switzerland

- ^b Also at An-Najah National University, Nablus, Palestine
- ^c Also at Borough of Manhattan Community College, City University of New York, New York, NY, USA
- ^d Also at Bruno Kessler Foundation, Trento, Italy
- ^e Also at Center for High Energy Physics, Peking University, Beijing, China
- ^f Also at Centro Studi e Ricerche Enrico Fermi, Rome, Italy
- ^g Also at CERN, Geneva, Switzerland
- ^h Also at Département de Physique Nucléaire et Corpusculaire, Université de Genève, Geneva, Switzerland
- ⁱ Also at Departament de Física de la Universitat Autònoma de Barcelona, Barcelona, Spain
- ^j Also at Department of Financial and Management Engineering, University of the Aegean, Chios, Greece
- ^k Also at Department of Physics and Astronomy, Michigan State University, East Lansing, MI, USA
- ^l Also at Department of Physics and Astronomy, University of Louisville, Louisville, KY, USA
- ^m Also at Department of Physics, Ben Gurion University of the Negev, Beer Sheva, Israel
- ⁿ Also at Department of Physics, California State University, East Bay, Long Beach, USA
- ^o Also at Department of Physics, California State University, Sacramento, USA
- ^p Also at Department of Physics, King's College London, London, UK
- ^q Also at Department of Physics, University of Fribourg, Fribourg, Switzerland
- ^r Also at Department of Physics, University of Thessaly, Greece
- ^s Also at Department of Physics, Westmont College, Santa Barbara, USA
- ^t Also at Hellenic Open University, Patras, Greece
- ^u Also at Institutio Catalana de Recerca i Estudis Avancats, ICREA, Barcelona, Spain
- ^v Also at Institut für Experimentalphysik, Universität Hamburg, Hamburg, Germany
- ^w Also at Institute of Particle Physics (IPP), Montreal, Canada
- ^x Also at Institute of Physics, Azerbaijan Academy of Sciences, Baku, Azerbaijan
- ^y Also at Institute of Theoretical Physics, Ilia State University, Tbilisi, Georgia
- ^z Also at Lawrence Livermore National Laboratory, Livermore, USA
- ^{aa} Also at III. Physikalisches Institut A, RWTH Aachen University, Aachen, Germany
- ^{ab} Also at The Collaborative Innovation Center of Quantum Matter (CICQM), Beijing, China
- ^{ac} Also at TRIUMF, Vancouver, BC, Canada
- ^{ad} Also at Università di Napoli Parthenope, Naples, Italy
- ^{ae} Also at University of Chinese Academy of Sciences (UCAS), Beijing, China
- ^{af} Also at Department of Physics, University of Colorado Boulder, Colorado, USA
- ^{ag} Also at Washington College, Chestertown, MD, USA
- ^{ah} Also at Physics Department, Yeditepe University, Istanbul, Türkiye
- * Deceased